

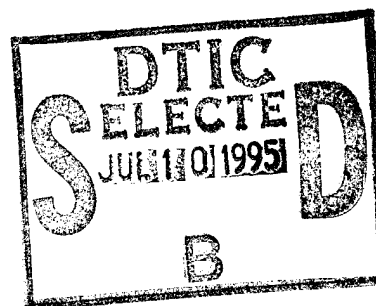
# NAVAL POSTGRADUATE SCHOOL

## Monterey, California



STANDARD COPY/NOT REPRODUCED  
EXCEPT BY THIS PROCESSING  
FACILITY IN BLACK AND  
WHITE

### THESIS



#### THE SPACE SHUTTLE ORBITER'S ADVANCED DISPLAY DESIGNS AND AN ANALYSIS OF ITS GROWTH CAPABILITIES

by

Baoquoc Tranthien

March 1995

Thesis Advisor:

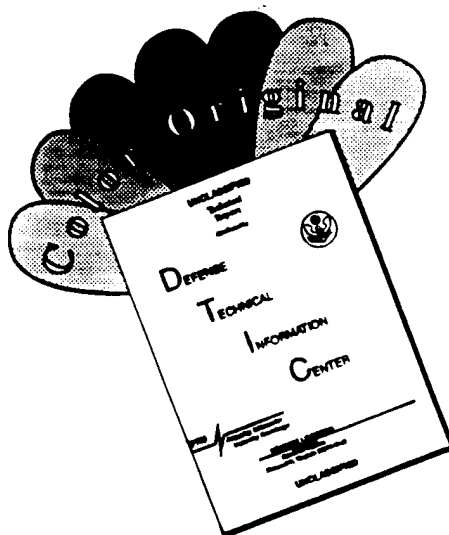
Wade Duym

Approved for public release; distribution is unlimited.

19950705 034

DTIC QUALITY INSPECTED 8

# DISCLAIMER NOTICE



THIS DOCUMENT IS BEST QUALITY AVAILABLE. THE COPY FURNISHED TO DTIC CONTAINED A SIGNIFICANT NUMBER OF COLOR PAGES WHICH DO NOT REPRODUCE LEGIBLY ON BLACK AND WHITE MICROFICHE.

REPORT DOCUMENTATION PAGE			Form Approved OMB No. 0704	
<p>Public reporting burden for this collection of information is estimated to average 1 hour per response, including the time for reviewing instruction, searching existing data sources, gathering and maintaining the data needed, and completing and reviewing the collection of information. Send comments regarding this burden estimate or any other aspect of this collection of information, including suggestions for reducing this burden, to Washington headquarters Services, Directorate for Information Operations and Reports, 1215 Jefferson Davis Highway, Suite 1204, Arlington, VA 22202-4302, and to the Office of Management and Budget, Paperwork Reduction Project (0704-0188) Washington DC 20503.</p>				
1. AGENCY USE ONLY (Leave blank)		2. REPORT DATE March 1995		3. REPORT TYPE AND DATES COVERED Master's Thesis, Final
4. TITLE AND SUBTITLE : THE SPACE SHUTTLE ORBITER's ADVANCED DISPLAY DESIGNS AND AN ANALYSIS OF ITS GROWTH CAPABILITIES			5. FUNDING NUMBERS	
6. AUTHOR(S) Tranthien, Baoquoc				
7. PERFORMING ORGANIZATION NAME(S) AND ADDRESS(ES) Naval Postgraduate School Monterey CA 93943-5000			8. PERFORMING ORGANIZATION REPORT NUMBER	
9. SPONSORING/MONITORING AGENCY NAME(S) AND ADDRESS(ES) NONE			10. SPONSORING/MONITORING AGENCY REPORT NUMBER	
11. SUPPLEMENTARY NOTES The views expressed in this thesis are those of the author and do not reflect the official policy or position of the Department of Defense or the U.S. Government.				
12a. DISTRIBUTION/AVAILABILITY STATEMENT Approved for public release; distribution unlimited			12b. DISTRIBUTION CODE	
13. ABSTRACT (maximum 200 words) This thesis analyzes the growth capability of the Space Shuttle Orbiter's Multifunction Electronic Display Subsystem (MEDS). MEDS is a new "glass cockpit" system, using Active Matrix Liquid Crystal Displays (AMLCD) to replace the existing Orbiter cockpit instruments. The primary goals were to analyze the MEDS growth capabilities and to propose advanced Orbiter displays using the MEDS. Analysis of the Orbiter state vectors resulted in designs for real-time graphical displays for use during the ascent, orbital entry and rendezvous phases of the mission.				
14. SUBJECT TERMS Space shuttle, Orbiter, Multifunction Electronic Display Subsystem (MEDS), Active Matrix LCD (AMLCD), National Aeronautics and Space Administration (NASA), Downrange Abort Evaluator (DAE), Matlab			15. NUMBER OF PAGES 71	
			16. PRICE CODE	
17. SECURITY CLASSIFICATION OF REPORT Unclassified	18. SECURITY CLASSIFICATION OF THIS PAGE Unclassified	19. SECURITY CLASSIFICATION OF ABSTRACT Unclassified	20. LIMITATION OF ABSTRACT UL	



Approved for public release; distribution is unlimited

**THE SPACE SHUTTLE ORBITER'S ADVANCED  
DISPLAY DESIGNS AND AN ANALYSIS OF ITS  
GROWTH CAPABILITIES**

by

Baoquoc Tranthien  
Lieutenant, United States Navy  
B.A., University of Washington, 1987

Submitted in partial fulfillment  
of the requirements for the degree of

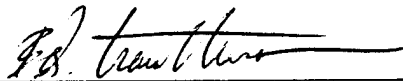
**MASTER OF SCIENCE IN ASTRONAUTICAL ENGINEERING**

from the

**NAVAL POSTGRADUATE SCHOOL**

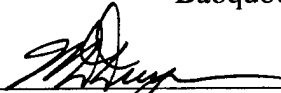
March 1995

Author:

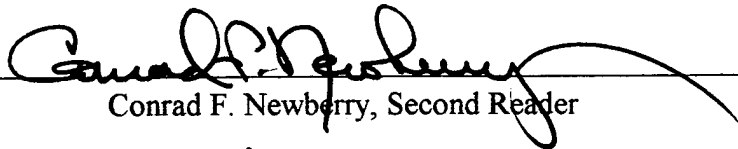


Baoquoc Tranthien

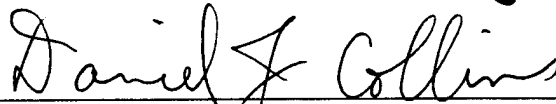
Approved by:



CDR Wade Duym, Thesis Advisor



Conrad F. Newberry, Second Reader



Daniel F. Collins, Chairman  
Department of Aeronautical/Astronautical Engineering

Accession For	
NTIS GRA&I	<input checked="" type="checkbox"/>
DTIC TAB	<input type="checkbox"/>
Unannounced	<input type="checkbox"/>
Justification	
By	
Distribution/	
Availability Codes	
Dist	Avail and/or Special
A-1	

## **ABSTRACT**

This thesis analyzes the growth capability of the Space Shuttle Orbiter's Multifunction Electronic Display Subsystem (MEDS). MEDS is a new "glass cockpit" system, using Active Matrix Liquid Crystal Displays (AMLCD) to replace the existing Orbiter cockpit instruments. The primary goals were to analyze the MEDS' growth capabilities and to propose advanced Orbiter displays using the MEDS. Analysis of the Orbiter state vectors resulted in designs for real-time graphical displays for use during the ascent, orbital entry and rendezvous phases of the mission.

## **THESIS DISCLAIMER**

The reader is cautioned that the computer programs SHUTTLE and INIT have not been exercised for all cases of interest. While every effort has been made within the time available to ensure that the programs are free of computational and logic errors, they cannot be considered validated. Any application of these programs without additional verification is at the risk of the user.





## TABLE OF CONTENTS

I. INTRODUCTION .....	1
A. GENERAL .....	1
B. SPACE SHUTTLE COCKPIT UPGRADE .....	1
C. EXPERIENCE TOUR .....	3
D. SCOPE .....	3
II. BACKGROUND .....	5
A. SPACE SHUTTLE'S MISSION REQUIREMENTS .....	5
B. EVOLUTION OF CURRENT AVIONICS SYSTEM .....	8
C. DISPLAY UPGRADE REQUIRED .....	10
III. MEDS IMPLEMENTATION .....	11
A. MEDS OVERVIEW .....	11
B. HARDWARE .....	11
1. General Purpose Computer (GPC) .....	11
2. Display Driver Unit (DDU) .....	12
3. Display Electronics Unit (DEU) .....	12
4. Integrated Display Processor (IDP) .....	15
5. Multifunction Display Unit (MDU) .....	16
6. Analog-to-Digital Converter (ADC) .....	18
7. Keyboard .....	19

C. SOFTWARE .....	19
D. FAULT TOLERANCE .....	19
E. TRADEOFFS .....	19
F. NEW MEDS DISPLAYS .....	20
IV. COCKPIT OPTIMIZATION .....	23
A. GROWTH OPTIONS .....	23
B. CREW PREFERENCES .....	23
C. GRID COMPUTER EXPERIMENT .....	24
D. PROPOSED INCORPORATION OF MEDS .....	25
1. Altering the Flight Software .....	26
2. PCMMU Link to the Primary Side of the IDP .....	27
3. PCMMU Link to the Auxiliary Side of the IDP .....	28
E. ASCENT ABORTS .....	29
F. ASCENT/DESCENT ADVANCED ORBITER DISPLAYS .....	30
V. DOWNRANGE ABORT EVALUATOR (DAE) .....	35
A. EQUATIONS OF MOTION .....	35
1. Reference Frame .....	36
2. Kinematics .....	36
3. Gravitational Force .....	37
4. Drag Force .....	37
5. Lift Force .....	38

6. Thrust Force .....	38
B. MATLAB PROGRAM .....	39
1. Space Shuttle 3 EO Case Study .....	39
C. DATA COMPARISON .....	42
1. Downrange Abort Evaluator (DAE) .....	42
2. Possible Output Differences .....	42
VI. CONCLUSIONS .....	45
A. OPTIMAL MEDS IMPLEMENTATION METHODS .....	45
A. FINAL PROPOSED DESIGN .....	46
B. RESULTS OF MATLAB VS. NASA'S DAE .....	46
C. RECOMMENDATIONS .....	46
LIST OF REFERENCES .....	47
APPENDIX A. MEDS HARDWARE SPECIFICATIONS .....	49
APPENDIX B. MATLAB PROGRAMS 'SHUTTLE' AND 'INIT' .....	53
INITIAL DISTRIBUTION LIST .....	59

## **I. INTRODUCTION**

### **A. GENERAL**

The purpose of a cockpit display system is to present pertinent aircraft information such as attitude, heading, altitude, airspeed, and engine status to the pilot. A well-designed flight deck takes into account space and human factors requirements to maximize the crew's ability to control the aircraft. Cockpit display media have evolved from simple needle and dial instruments to current state-of-the-art color multifunction Liquid Crystal Displays (LCDs). These computer-generated displays use high speed microprocessors and have few limitations to the types of graphical displays that can be depicted. [Refs. 1 and 2]

### **B. SPACE SHUTTLE COCKPIT UPGRADE**

The Space Shuttle program is in the process of upgrading its fleet with a new display subsystem, the Multifunction Electronic Display Subsystem (MEDS), using color Active Matrix Liquid Crystal Displays (AMLCDs). The driving factors in the upgrade are the obsolescence of the Shuttle Orbiter's current Cathode Ray Tube (CRT) displays and the difficulty of maintaining the electromechanical cockpit instruments.

Rockwell International, Downey, California, is the prime contractor with Honeywell Inc., Space System Division, as the major subcontractor. There are two separate contracts for development and for production supporting the planned first launch with the MEDS in July 1998. The \$59.3 million Design, Development, Test, and Evaluation (DDT&E) contract includes the qualification of hardware and software, integration and verification testing at Johnson Space Center (JSC) laboratories. The \$85.2 million production contract includes the fabrication and assembly of modification kits, flight and nonflight Line Replacement Units (LRUs), and the procurement of spare Shop Replacement Units (SRUs) and piece parts. Production began in March 1994 and will

continue to the end of February 1998. The software architecture and organizational responsibilities are divided among Rockwell and Honeywell as shown in Fig. 1.1. [Ref. 3]

A Preliminary Design Review (PDR) and a Critical Design Review (CDR) were successfully completed in May 1993 and February 1994, respectively. As of May 1994, the LRU's engineering models were completed, a single string test verified that the LRU could communicate via a MIL-STD-1553B data bus, the first production AMLCD panels were delivered to Honeywell, the hardware dependent software design was 95% complete, the display format design was 100% complete, and the configuration control board was baselined. [Ref. 3]

The plan by National Aeronautics and Space Administration (NASA) is to mimic the current cockpit display to minimize crew training impacts during the mixed fleet operations period from 1998 to the year 2000. However, an Advanced Orbiter Display working group was formed in August 1994 to plan for the full utilization of MEDS. The purpose of the working group is to implement the advanced capabilities of MEDS and develop new display formats by the year 2002. The working group consists of representatives from JSC's Orbiter Project Office, the Astronaut's Office, Langley

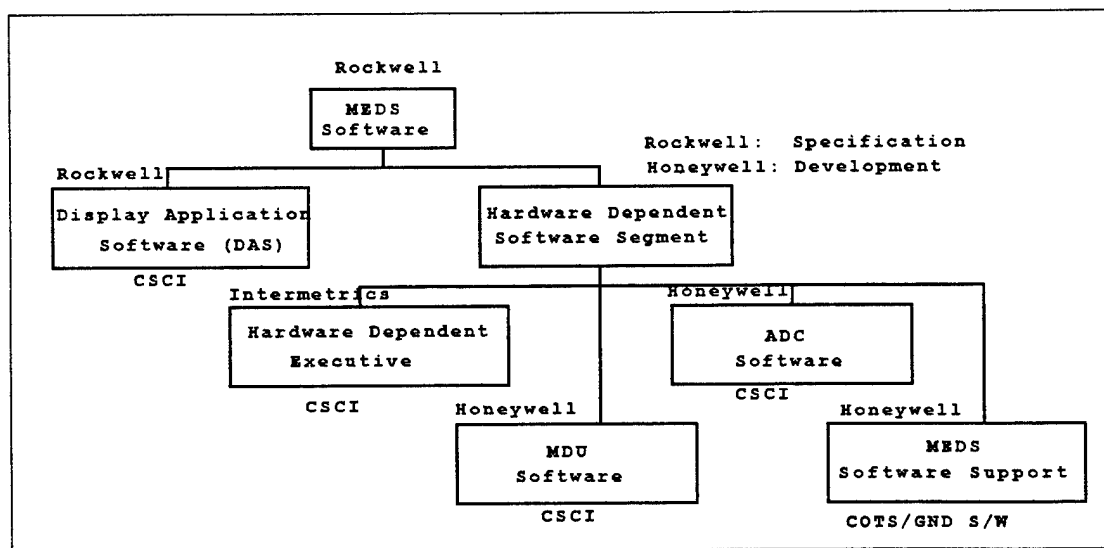


Figure 1.1. MEDS Software Architecture & Organizational Responsibilities. (After Ref. [3])

Research Center (LaRC), Ames Research Center (ARC), Honeywell, and Rockwell. [Ref. 3]

### **C. EXPERIENCE TOUR**

The Naval Postgraduate School (NPS) gives students the opportunity to do a thesis related experience tour during the course of their studies. The author spent the Spring of 1994 at JSC, Houston, researching and developing system architecture and hardware requirements for future utilization of the MEDS growth capability. System schematics to link the Shuttle's primary data with MEDS were developed with the assistance of JSC's engineers and three Astronauts: Kent Rominger, Chris Hadfield, and Brent Jett. Preliminary sketches of future display formats were discussed; more details will follow in later chapters of this thesis.

### **D. SCOPE**

The intent of this thesis is to explore the MEDS' growth capabilities, provide alternative methods for incorporating data into MEDS, design proposed displays for use during ascent and entry phases of flight, and to analyze the Orbiter's state vector which resulted in designs for real-time graphical displays.

Chapter II provides a detailed background description of the Space Transportation System (STS) and identifies the Space Shuttle's mission requirements. A description of the evolution of the current cockpit shows that it resulted from experience with previous space vehicles and technologies available in the seventies. Chapter II also lists reasons for the need to upgrade the Shuttle's cockpit.

Chapter III contains an explanation of what MEDS entails. The explanation contains a discussion of the software and hardware required, then identifies the various avionics components that MEDS will replace. The implementation of MEDS will result in significant weight and power savings. Major design tradeoffs are discussed.

Chapter IV focuses on cockpit displays optimization and the proposed advanced orbiter display. There are several options in the implementation of MEDS, each with its

advantages and disadvantages. The validation process and lead time for primary flight software provoke resistance to changes in the software codes. By using the auxiliary backplane of the IDP and the downlist information available through the Pulse-Code Modulation Master Unit (PCMMU), real-time flight data can be made available to the MEDS. The proposed ascent display developed by the author, which can also be use as an entry display, is shown at different times to simulate the dynamics of the problem. With feedback from the Astronaut's Office at JSC, the proposed design is depicted.

Chapter V contains data which suggest that by analyzing the orbiter's state vector, a real-time graphical display design is possible. By performing a numerical analysis of the governing equations of motion, a vehicle's impact point can be predicted. The numerical analysis shows that this analysis can be done on personal computer (PC) by writing a simple Matlab program. A special case of the three engine out abort mode is analyzed and the result is compared with NASA's Downrange Abort Evaluator (DAE) result. The comparison showed that a PC can be use to emulate the MEDS processing capabilities.

Chapter VI contains conclusions and recommendations for future thesis topics.

## **II. BACKGROUND**

The Space Shuttle, developed by NASA and Rockwell International, represents a significant advance in technology. Rockwell International was responsible for building the orbiter and integrating the Space Transportation System (STS). Numerous engineering and manufacturing contractors were also responsible for building subsystems for the STS.

### **A. SPACE SHUTTLE'S MISSION REQUIREMENTS**

The basic mission consists of lift-off in a vertical (nose-up) position from NASA John F. Kennedy Space Center (KSC), ascent and insertion into low Earth orbit, performance of payload operations, and descent to an unpowered landing on a 15000 foot runway. The primary landing sites are KSC and Edwards Air Force Base. Alternate landing sites with 8000 foot runways can be used in case of an emergency. [Ref. 4]

As shown in Fig 2.1, the Space Shuttle system consists of four primary elements: an Orbiter spacecraft, two Solid Rocket Boosters (SRBs), an External Tank (ET) for the fuel and oxidizer, and three Space Shuttle Main Engines (SSMEs). The Shuttle payloads, carried in a bay 60 feet long and 15 feet in diameter, can be launched into a circular low earth orbit of 185 to 570 kilometers. The maximum payload capability is a function of the Shuttle altitude and inclination of the orbit. The orbiter can accommodate up to eight flight crew members for a nominal mission length of 4 to 16 days in space. Other STS requirements include reuse of the orbiter and SRBs and limiting the orbiter's acceleration load to less than 3 g's. [Refs. 4 and 5]

A typical Space Shuttle launch profile is illustrated in Fig. 2.2. The total thrust at lift-off provided by the three main engines and the two SRBs is 6,425,000 lbs. The three main engines provide a total of 1,125,000 lbs of thrust by burning liquid oxygen and liquid hydrogen fuel from the external tank. The main engines are augmented by two solid rocket boosters, which burn out approximately two minutes after launch at an altitude of 43 km. The boosters are jettisoned, parachuted into the ocean, and recovered by ships for reuse in later launches. The orbiter and ET continue to ascend using the thrust of the



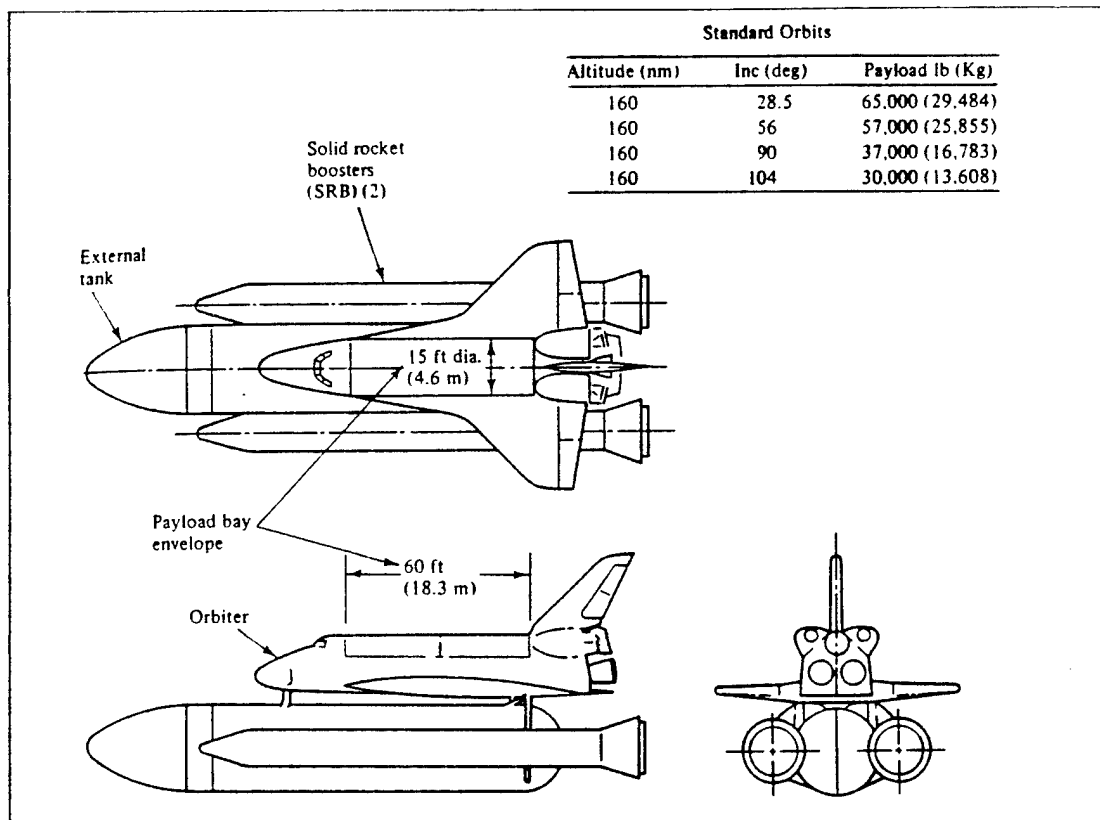


**Figure 2.1. Space Shuttle system. (From Ref. [5])**

three SSMEs. The SSMEs are shut down (main engine cutoff or MECO) just short of orbital velocity. The ET is jettisoned at MECO, approximately eight minutes after launch and at an altitude of 115 km, and is burned up as it reenters the atmosphere. At this critical point of the launch, the Reaction Control System (RCS) stabilizes the orbiter until the Orbiter Maneuvering System (OMS) can place the orbiter into a circular parking orbit. While on orbit, the crew performs mission objectives, such as satellite deployment or retrieval and various scientific experiments. When orbital operations are completed, the RCS and OMS are used to reorient and slow the orbiter for deorbit and re-entry. The RCS controls the attitude of the orbiter at re-entry by augmenting the aerodynamic control surfaces. This continues until atmospheric density is sufficient for the control surfaces to become fully effective. There is a period of a few minutes, called blackout, where all communications from the Shuttle are lost during the entry phase. During entry, the

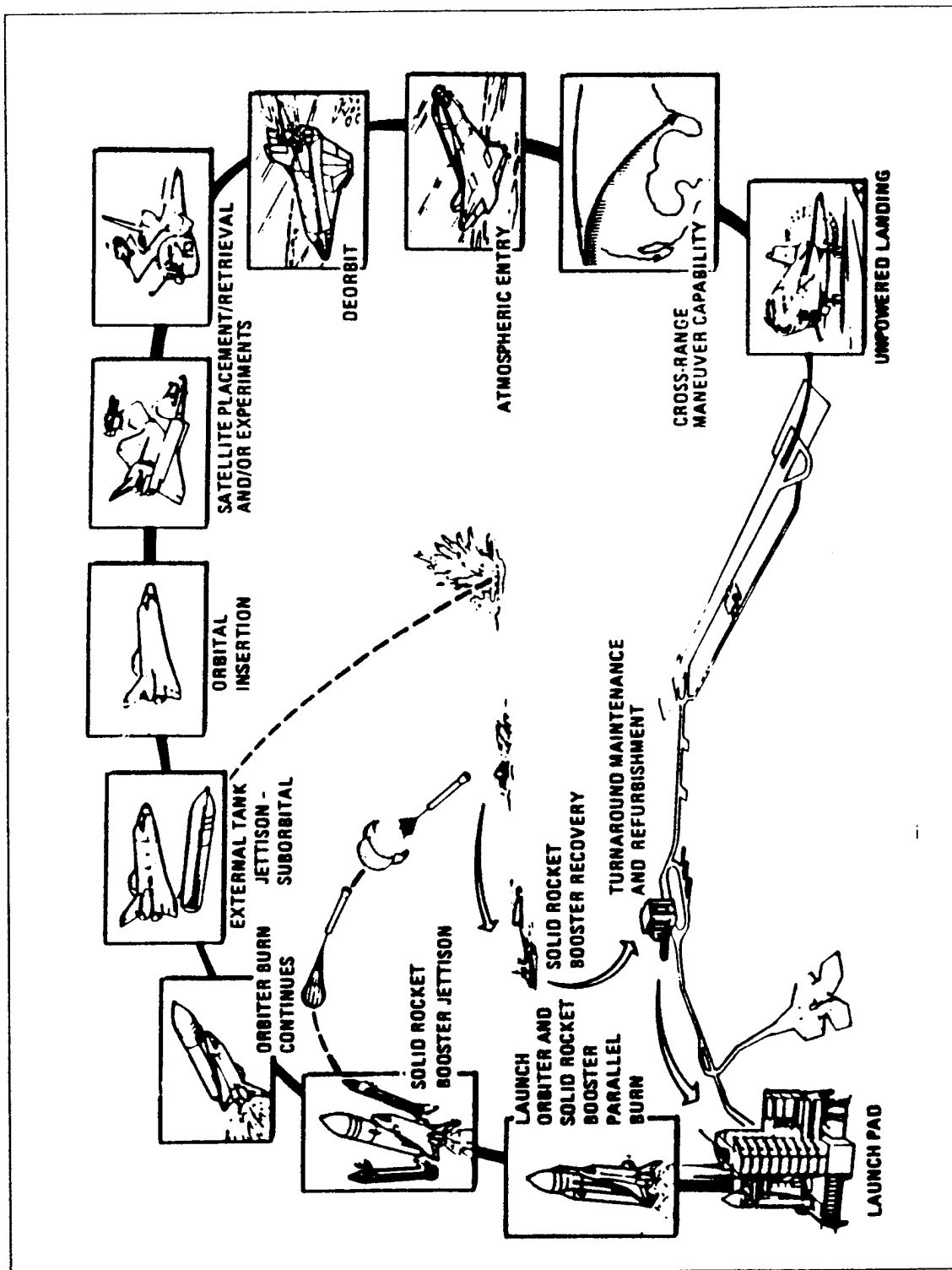


Figure 2.2. Typical Space Shuttle launch sequence. (From Ref. [5])

Orbiter's speed is decreased by energy dissipation due to atmospheric drag. As the Orbiter approaches the landing site, excess energy is dissipated by performing S-turns to slow the vehicle even more. Without power, there is no go-around capability, so the Orbiter only has one chance for a controlled landing. [Ref. 4]

## **B. EVOLUTION OF CURRENT AVIONICS SYSTEM**

The Space Shuttle avionics system is the result of years of studies, development, testing, and analysis conducted by NASA and various contractors. To understand the configuration and makeup of the Shuttle, the design environment of the early seventies must be understood. During this period of time the functions of switches, push-buttons, and input devices were usually hardwired to the box or subsystem. Displays were generally mechanical, hardwired, and served the dedicated function. Electronically driven horizontal and vertical situation displays utilized a mechanical representation. Electronic attitude and directional indicators were just emerging and were not commonly used. Heads-up displays (HUDs) were also just emerging. The concept of multifunction displays had never been used in an aerospace application and the design issue of a redundant system for display had never been addressed. The current orbiter's cockpit is depicted in Fig 2.3. [Ref. 4]

It was a major challenge for the designers to integrate all the displays required to operate the orbiter and its subsystems into the space available. All of the switches and displays had to be within reach and visible to the crew. Some of the requirements imposed were: safe return with a single crewman from either forward station; normal operation, except payload management, with a crew of two; accessibility from the two forward stations of all controls and displays required for ascent and entry; provisions for manual override of automated critical functions; and means to annunciate faults in and to command safing of hazardous systems. [Ref. 4]

The significant difference between the Space Shuttle mission and previous manned space programs is that the system would have to provide for both space flight and aircraft aerodynamic flight. In early design phases, considerations were given to incorporate two

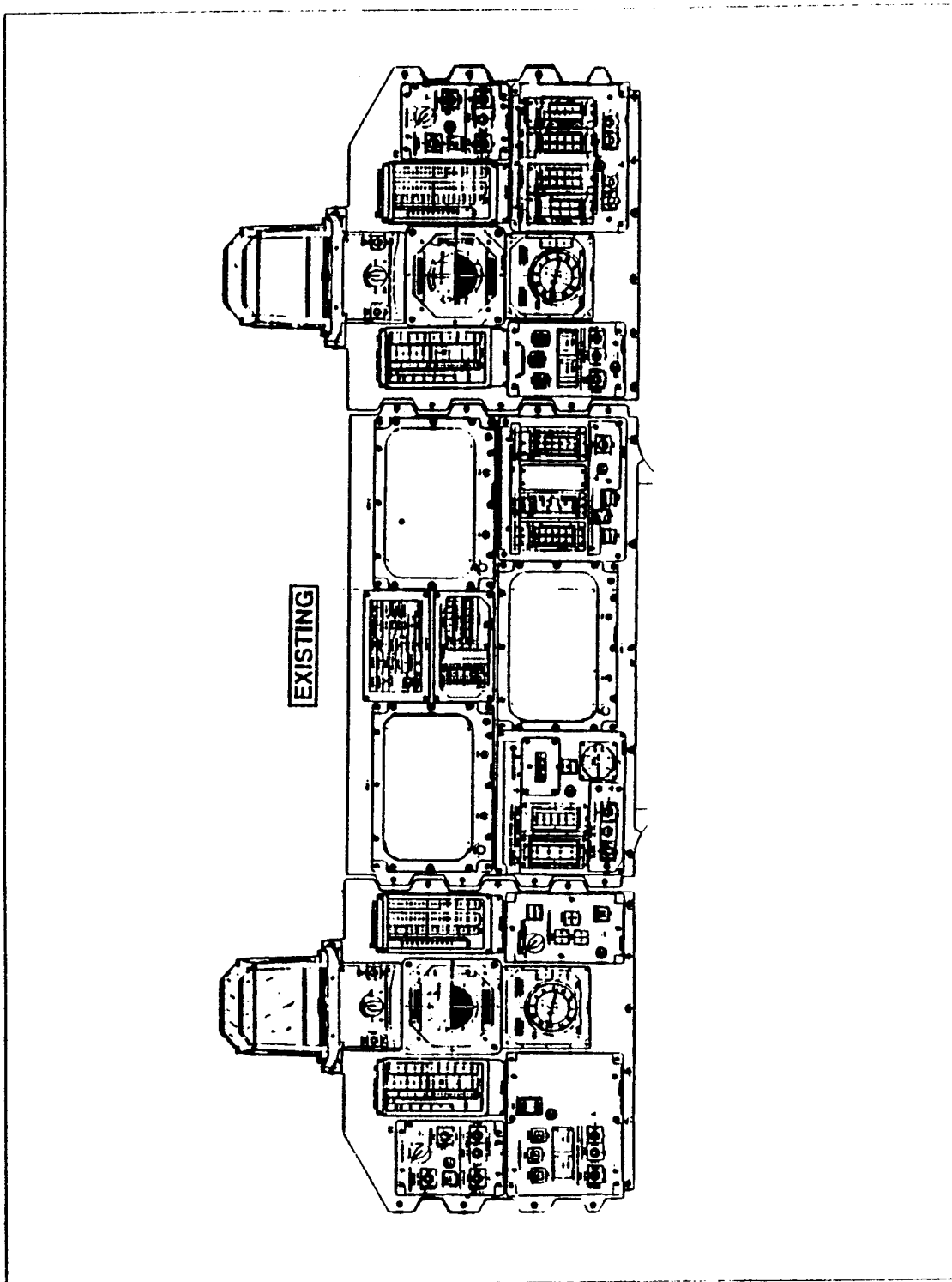


Figure 2.3. Current Space Shuttle cockpit. (From Ref. [5])

separate cockpits for the two flight modes. However, a single, integrated, two-man forward station was baselined for both regimes. The aft portion of the cockpit was equipped with controls and displays for on-orbit proximity and payload operations. From the aft cockpit's windows vantage point, the payload bay and aft view are clearly visible. The aft cockpit served its purpose effectively for satellite operations. Most of the displays in the cockpit served a dual purpose, but some, such as air data, the radar altimeter and navaid displays, became effective only after blackout during entry. It was decided that the leading edge of technology off-the-shelf system would be used wherever possible. The system which evolved consists of: control devices including toggle, push-button, thumbwheel, and rotary switches; potentiometers; multifunction keyboards; and circuit breakers. Displays included circular and vertical meters, tape meters, flight control meters, annunciators, electromechanical position and attitude indicators, digital readouts, and multifunction Cathode Ray Tubes (CRTs). [Ref. 4]

### **C. DISPLAY UPGRADE REQUIRED**

There have been few changes to the cockpit of the orbiter since the first launch of the Space Shuttle Columbia on 12 April 1981. The Space Shuttle is still one of the most intricate and complex aircraft/spacecraft to date, but its cockpit avionics is obsolescent. The primary reason for upgrading the cockpit is aging and wear of the electromechanical devices. The obsolescence of these parts and the high maintenance costs of the CRTs drove the Space Shuttle program to update the CRTs display subsystem, flight instruments, and system meters subsystem. [Ref. 4]

The upgrade to the Multifunction Electronic Display Subsystem (MEDS) will increase the capabilities of the display system, enhance flight safety, decrease the repair cost and decrease turnaround time. By using solid-state technology and space qualified avionics components, the system reliability will increase and susceptibility to electromagnetic interference will decrease. The modularity and use of shop replacement unit (SRU) parts will enhance the maintainability on the ground and in-flight. Another benefit of the new MEDS system is significant power and weight savings.

### **III. MEDS IMPLEMENTATION**

#### **A. MEDS OVERVIEW**

The Multifunction Electronic Display Subsystem (MEDS), sometimes referred to as a glass cockpit, is a state-of-the-art integrated display system which consists of four Integrated Display Processors (IDPs), four Analog-to-Digital Converters (ADCs) and eleven Multifunction Display Units (MDUs). The MEDS architecture is interconnected via a MIL-STD-1553B databus network. MEDS replaces the current Orbiter electromechanical flight instruments, servo-driven tape meters, the monochrome CRT displays and their associated electronics units. The new MEDS system is transparent to the existing orbiter's General Purpose Computer (GPC) software and interconnecting subsystems. To get a better understanding of what is being replaced by MEDS, a block diagram of the existing dedicated display system is shown in Fig. 3.1. The MEDS architecture is shown in Fig. 3.2, from Ref. 6, and the new glass cockpit (MEDS) is depicted in Fig. 3.3.

#### **B. HARDWARE**

##### **1. General Purpose Computer (GPC)**

The heart of the Shuttle's avionics is the General Purpose Computer with 256K of random access memory (RAM). There are five GPCs, all of which are identical IBM AP-101S machines. Each GPC contains the central processing unit (CPU), the input/output processor and the memory. During the critical phases of the mission, such as ascent and entry, four of the GPCs are loaded with the same Primary Avionics System Software (PASS) and operate redundant to each other. The fifth GPC is loaded with the Backup Flight System (BFS) software capable of communicating with all buses for mission completion or safe return from any point during the mission. The GPC is part of the old avionics system and it is not being replaced by the incorporation of MEDS. [Refs. 4 and 7]

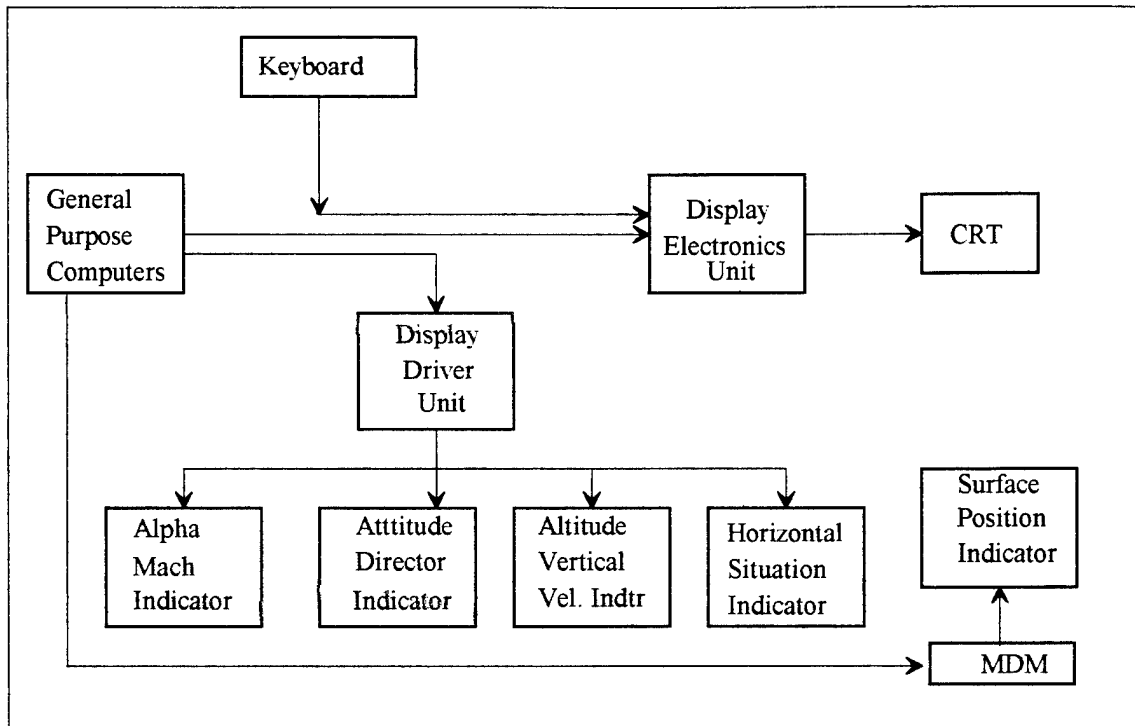


**Figure 3.1. Existing Dedicated Display system. (After Ref. [7])**

## **2. Display Driver Unit (DDU)**

The DDU is an electronic mechanism that connects the GPCs and the primary flight displays. It receives data signals from the computers and decodes them to drive the dedicated displays. The unit also provides dc and ac power for the Attitude Director Indicator (ADI) and the rotational and translational hand controllers. It contains logic for setting system failure flags on the dedicated instruments for such items as data loss and sensor failures. The orbiter contains display driver units at three locations: at the commander's flight station, the pilot's flight station, and the aft flight station. With the incorporation of MEDS, the DDU remains as part of the orbiter's avionics system for the sole purpose of providing power to the hand controller. [Refs. 4 and 7]

## **3. Display Electronics Unit (DEU)**

The DEU drives the general-purpose CRTs and accepts data inputs from the alphanumeric keyboard. Each DEU contains an IBM SP-0 special-purpose processor with

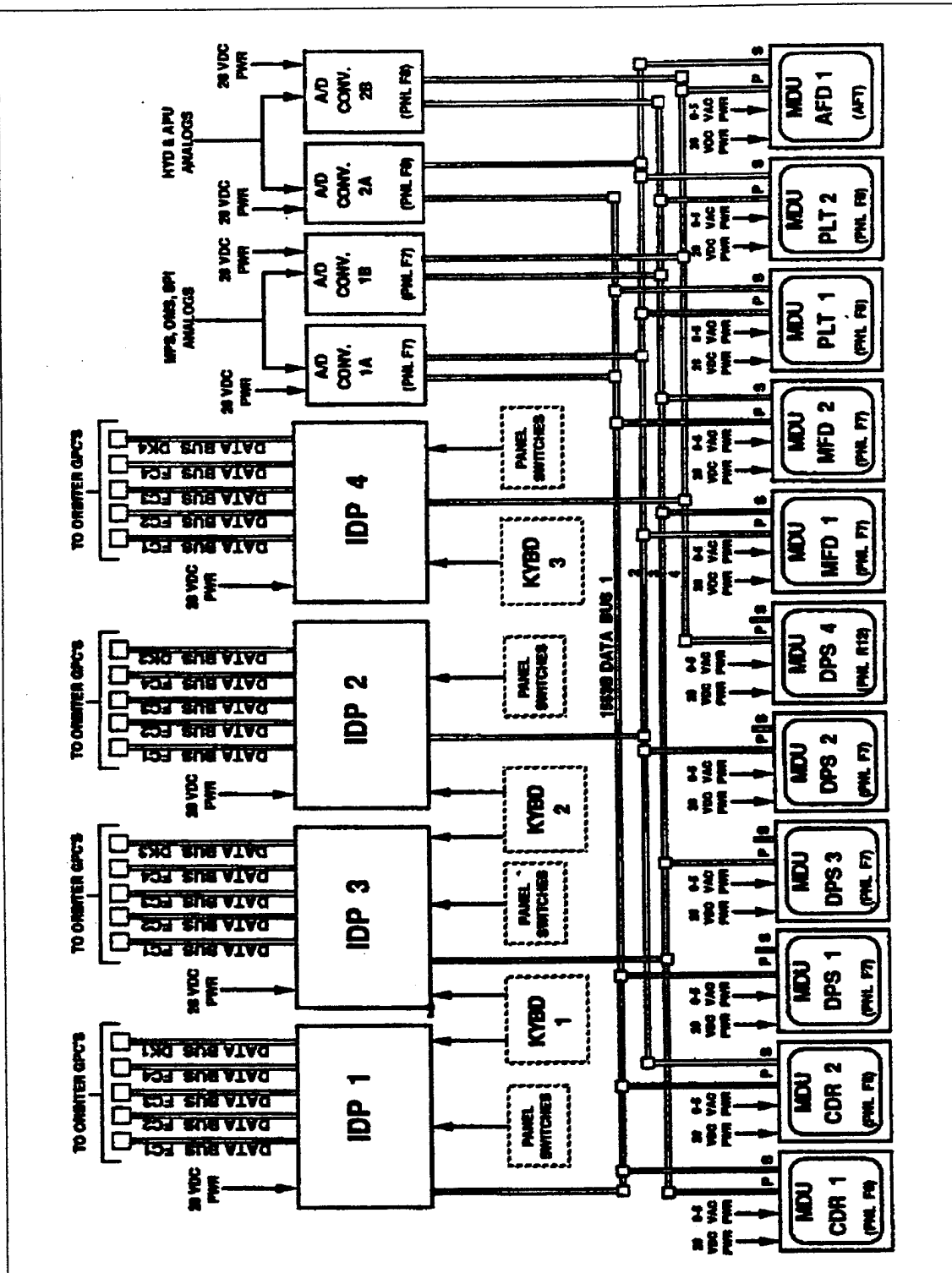


Figure 3.2. MEDS Architecture. (From Ref. [6])



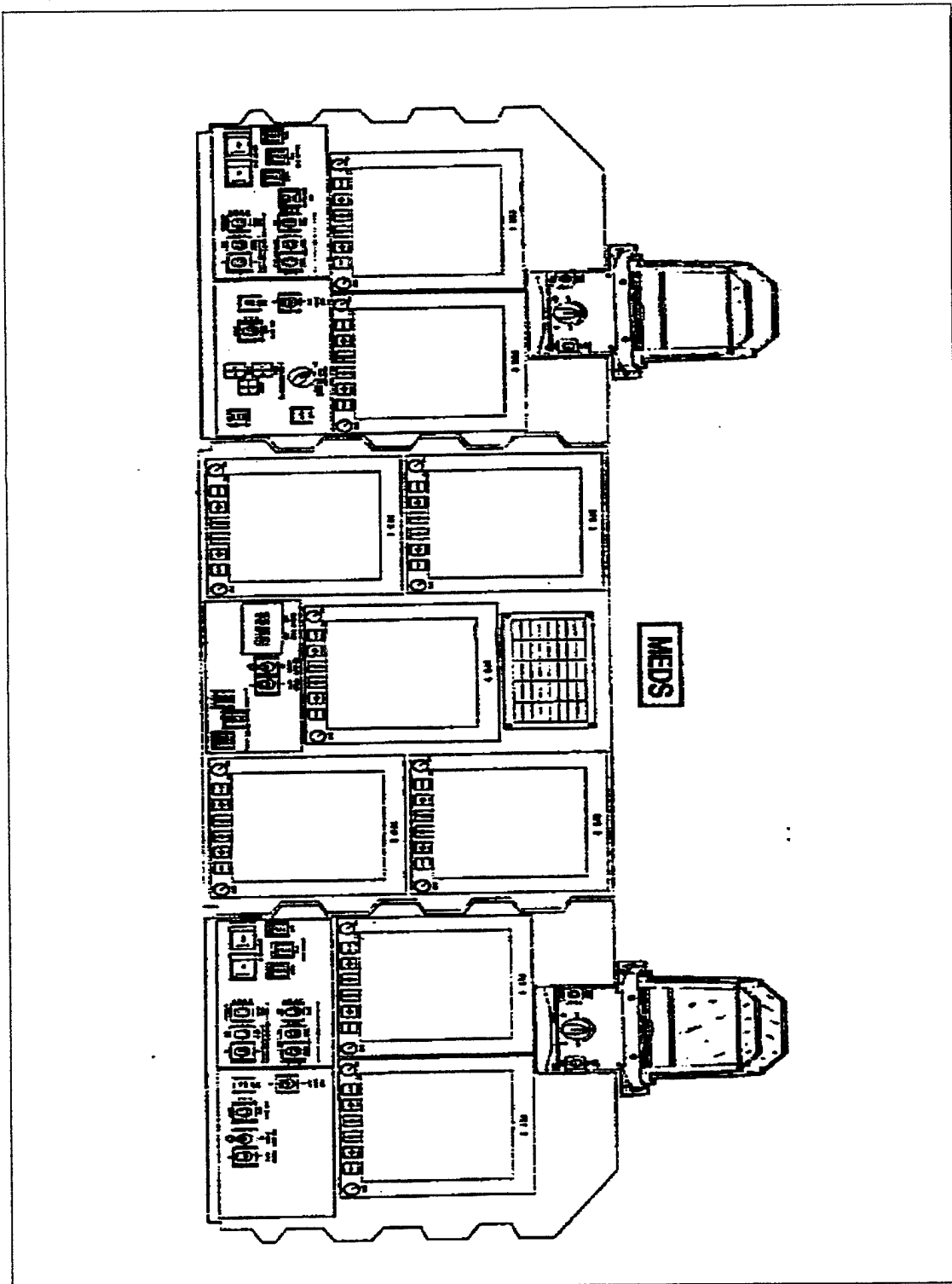


Figure 3.3. MEDS forward flight panel. (From Ref. [6])

8K of RAM (16-bit words) used to store critical CRT formats. Dynamic (flight) data are provided by the GPCs and integrated into the static format by the DEU. The DEU detects a keystroke, evaluates it for validity, and if valid, transmits the data to the GPC. [Refs. 4 and 7]

#### **4. Integrated Display Processor (IDP)**

The IDP is the heart of the MEDS system. The IDP replaces the existing orbiter Display Electronic Units as well as the Dedicated Display Units and will assume all the display processing control functions of the MEDS. The IDP is the interface between the MEDS and the orbiter's GPCs. The IDP contains a power converter unit to convert the orbiter supplied 28 VDC power to internal operating voltages as required. The IDP has its own CPU, volatile (loss in case of a power disruption) and non-volatile main memory, and non-volatile mass memory storage of 300 megabytes. It houses all of the MEDS required Display Applications Software. For communication with the orbiter's Display/Keyboard (DK) and Flight Critical (FC) data busses the IDP contains standard orbiter Multiplex Interface Adapters (MIAs). For communication with MEDS LRUs the IDP contains standard 1553B I/O ports. The IDP contains interface electronics to receive inputs from the orbiter keyboards, panel switches and Built-In Test Equipment (BITE). For future growth considerations, the IDP contains additional MIA and 1553B I/O ports. The IDP has two physically isolated DX backplanes consisting of the MEDS DX backplane and the auxiliary DX backplane. The split DX backplane provides physical isolation between critical display functions and non-critical mission-dependent functions. Figure 3.4 depicts the split DX backplane architecture.

The General Purpose Processor (GPP) is the heart of the IDP. The GPP is a 386DX microprocessor rated at 25 MHz, but is only operated at approximately 16 MHz. The GPP uses 32-bit registers, eight general purpose 32-bit registers, and 32-bit data paths. The GPP has four levels of user protection which provide application and operating system isolation. For increased processing performance the 386DX uses pipelined instruction execution and address translation caches. It is Electromagnetic

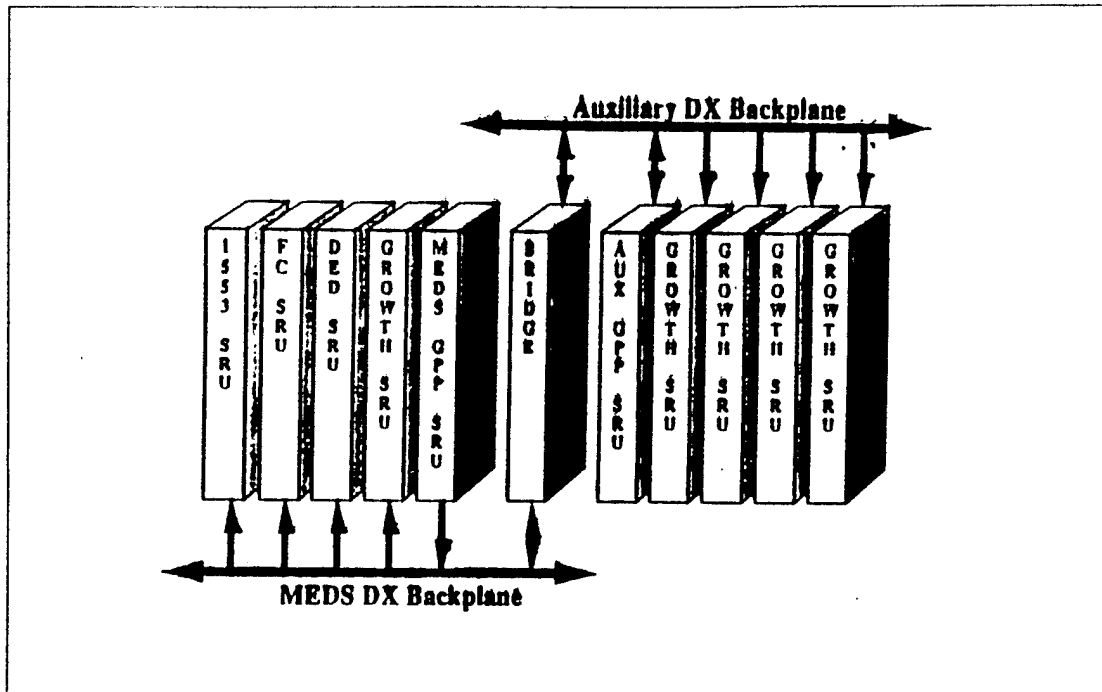


Figure 3.4. IDP Split DX Backplane Architecture. (From Ref. [6])

Interference (EMI) hardened and can support an optional 387DX math coprocessor; see Appendix A for specifications. [Refs. 6 and 8]

### 5. Multifunction Display Unit (MDU)

The MDU replaces the existing orbiter Display Units (CRT) and the Guidance Navigation and Control (GN&C) dedicated display electromechanical flight instruments: Attitude Direction Indicator (ADI); Alpha Mach Indicator (AMI); Altitude Vertical Velocity Indicator (AVVI); and Horizontal Situation Indicator (HSI). The following servo-driven and vertical tape meters are also being replaced: Main Propulsion System (MPS); hydraulics; Auxiliary Power Unit (APU); Surface Position Indicator (SPI); and the Orbital Maneuvering System (OMS). The MDU contains a power converter unit, a CPU, volatile and non-volatile memory and BITE. For communication with the IDP, the MDU contains a standard 1553B I/O port. The MDU has the capability to support NTSC/RS-170 video signals. Nine MDUs are located in the forward flight station and two in the aft flight station. [Refs. 6 and 8]

The MDU uses the state-of-the-art Active Matrix Liquid Crystal Display (AMLCD) format. The AMLCD display architecture is used with a Reduced Instruction Set Computer (RISC) processing element and custom graphics accelerator that produces two- and three-dimensional (2-D and 3-D) fully anti-aliased graphical images. Anti-aliasing filters are responsible for converting the 576 x 576 Video RAM (VRAM) image into the 1152 x 1152 addressability required by the LCD. An active display area of 6.71 x 6.71 in. is achieved with 1152 x 1152 pixels resolution and 28 shades of gray per primary color. A cutaway view of an AMLCD display is shown in Fig. 3.5.

A LCD consists of a liquid crystal substrate of long organic crystal threads which can be altered by applying electrical fields. The MDU uses Twisted Nematic (TN) threads which are twisted and change from reflective to transmissive when charged. The MDU uses an active matrix LCD technology. An Active matrix LCD uses an active element, usually an amorphous-silicon thin-film-transistor (a-Si TFT), located at each pixel. The pixel is addressed by rows and columns and stays on until it is switched off. This scheme

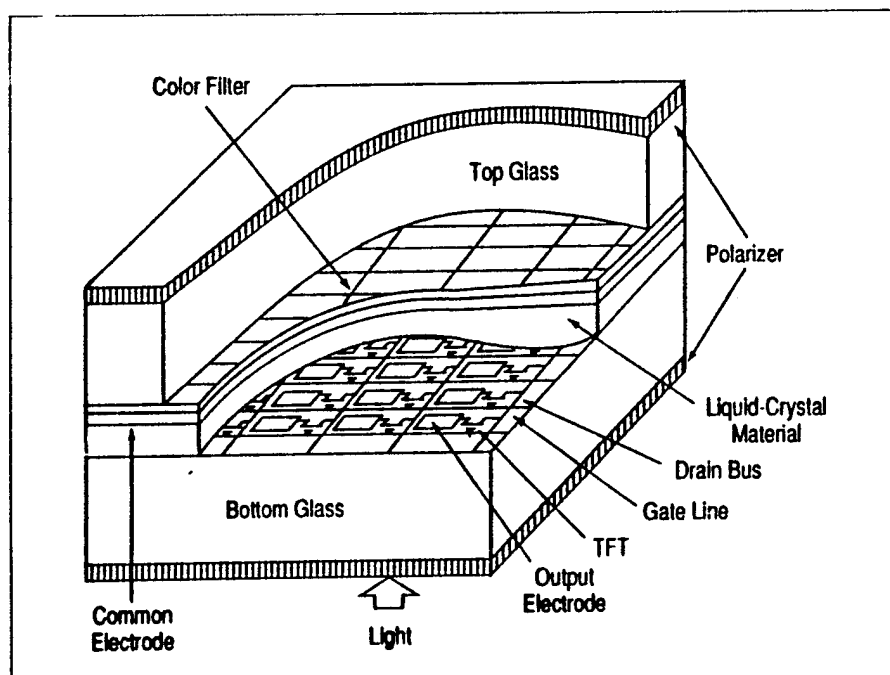


Figure 3.5. Active Matrix LCD. (From Ref. [1])

can refresh (update) the video screen at 60-Hz video rate. The latest accomplishment in AMLCD is a significant improvement in viewing angle. The viewing angle is defined as the angle between the screen's normal vector and the vector from the screen to the viewer's eyes. The MDU uses a newly implemented technique which controls the optical retardation in all three display axes by adding a retardation film. The film is designed with less birefringence parallel to the display surface than normal to it, which compensates for the increased optical path length through the display cell when the cell is viewed from off the normal. Another technique - the halftone/gray-scale method- achieves a wide viewing angle by dividing the pixel electrode to create subpixels, each of which sees a different voltage, using a capacitor divider circuit. The liquid crystal material at each subpixel is thus at a different state of rotation, and the complete pixel exhibits a wider viewing angle. These techniques along with the anti-aliasing which can program and control the color of each dot minimizes visually detectable image distortions. Active matrix requires placing thousands of TFTs on a glass substrate and if one of these TFT or a pair of electrodes are defective, it can ruin the entire panel. Honeywell and Optical Imaging System (OIS), Troy, Michigan are the developers for the AMLCD used by the MEDS system; see Appendix A for specifications. [Refs. 8 and 14]

## **6. Analog-to-Digital Converter (ADC)**

The ADC provides the Integrated Display Processor (IDP) with the converted digital data from analog instruments (MPS, HYD, APU, OMS, and SPI) for processing before it is sent to the Multifunction Display Unit (MDU) for display. It contains a power converter unit, a CPU, BITE and volatile & non-volatile memory. It also houses Analog-to-Digital converter electronics sufficient to convert 32 differential analog inputs to digital formats. For communication with the IDP, the MDU uses a standard 1553B I/O port. The ADC is an essential piece of hardware acquired for the new MEDS system; see Appendix A for specifications. [Ref. 8]

## **7. Keyboard**

The existing keyboard will be used with the new MEDS system. It is the primary interface for the crew and the IDP. There are three keyboards in the orbiter. Two are located in the center floor console of the forward cockpit and one in the aft cockpit. [Ref. 8]

## **C. SOFTWARE**

The MEDS software resides in the MEDS hardware (IDP, MDU, ADC) and consists of an operating system kernel and applications. The MEDS software are broken down into two categories, Hardware Dependent Software (HDS) and Display Application Software (DAS). The HDS is software that is hardware dependent considered as Operating System Kernel (OSK). The DAS is software that is use for display purposes and referred to as application software. [Ref. 8]

## **D. FAULT TOLERANCE**

MEDS requires a high level of reliability since it is a critical subsystem of the orbiter. The MEDS architecture incorporates a four string design in order to achieve two system level fault tolerance. After sustaining two successive failures, MEDS retains the capabilities to: maintain data display and GPC command interface adequate for a safe return to earth; display an adequate set, in graphical format, of flight instrument parameters at both of the forward flight stations; and display the assigned set of subsystem status parameters at (as a minimum) one of the forward flight stations. The power received for the orbiter Electrical Power Distribution and Control (EPD&C) subsystem is distributed such that, after sustaining two successive failures (including main dc bus failures), MEDS retains the display capabilities required for a safe return to earth. [Ref. 8]

## **E. TRADEOFFS**

A major advantage of implementing MEDS is the tremendous savings in weight and power required. A total savings of 84.9 lbs and 169 watts is achieved with MEDS. This weight directly translates to more payload that the Shuttle can carry. Some of the

mechanical switches were replaced by the edge keys on the MDUs. It will cost less to maintain the new MEDS avionics compared to the old electromechanical gauges and CRTs. From a crew training point of view, a very shallow learning curve is required due to the fact that MEDS mimics the cockpit displays of the existing Shuttle Orbiter cockpit.

One major concern with MEDS is the AMLCD that is used with the MDUs. This is the only component that has very little operational history. The MDU is the pivotal human interface portion of MEDS. The color AMLCD contains a liquid crystal screen and a 30 watt cathode fluorescent lamp in a sealed volume. If either fails, the MDU is useless.

#### **F. NEW MEDS DISPLAYS**

Some draft design formats are shown in Fig. 3.6 and 3.7. These designs are very close to the final product since they have been through crew evaluation and human factors analysis. Figure 3.6 shows a composite display with the ADI, HSI, AVVI and other instruments showing. Figure 3.7 shows an ADI/AVVI display format.

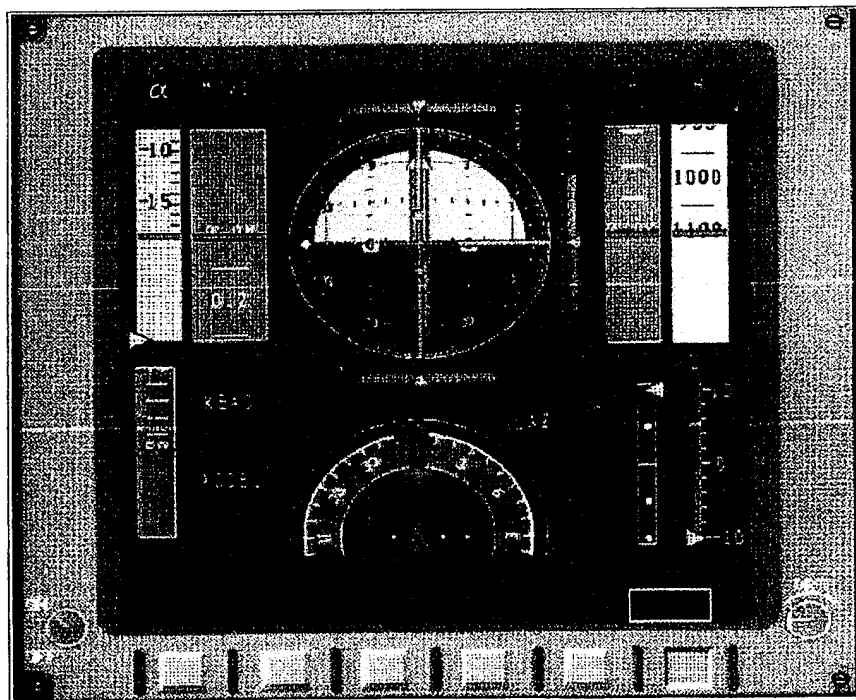


**Figure 3.6. Composite MEDS Display.**

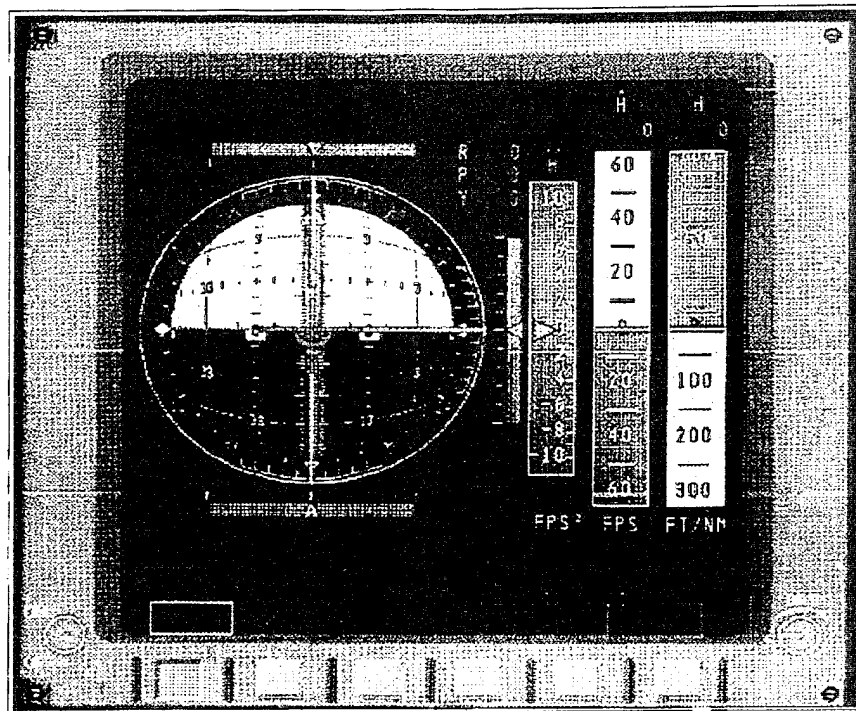


Figure 3.7. MEDS ADI/AVVI Display.





## **IV. COCKPIT OPTIMIZATION**

This chapter identifies Multifunction Electronic Display Subsystem (MEDS) growth options, crew preferences, optimization methods, and the result of a proposed advanced Orbiter display. The optimization methods are further explained by analyzing an ongoing NASA experiment which uses a laptop computer to depict relative motion. By incorporating MEDS, the relative motion plot and a new proposed ascent/descent plot can now be display via MEDS vice a laptop computer.

### **A. GROWTH OPTIONS**

Six spare slots in the Integrated Display Processor (IDP) are available for future upgrades to MEDS. The IDP unit is similar to a personal computer where extra cards can be added or replaced to the spare slot, to improve its speed and power. There are few limitations as to the type of cards that can be added to the IDP. The 80386 radiation hardened microprocessor can be replaced by a faster radiation hardened microprocessor if required. Multiple CPUs can also be added to the IDP as an option. Random Access Memory (RAM) can also be increased. For growth provisions, 200% processor throughput margin and 300% main memory margin are included in the current MEDS configuration.

### **B. CREW PREFERENCES**

At the first Advanced Orbiter Display working group meeting the crew proposed that MEDS be optimized as follows: optimize the flight instruments and systems management displays and formats; include checklists for critical malfunctions and standard cockpit layouts for each phase of flight; and incorporate additional data such as Pulse-Code Modulation Master Unit (PCMMU) data into MEDS to provide insight into flight state and systems status. These new displays would be beneficial during time critical and communications failure situations. [Ref. 9]

### C. GRID COMPUTER EXPERIMENT

An experiment by NASA uses PCMMU data to determine relative motion between the Space Shuttle and a target satellite. The experiment shows that data from the PCMMU can be used to give the flight crew real-time flight data via laptop computers. The relative motion displays used on the laptop were developed by Naval Postgraduate School (NPS) students; see Ref. 10. An advantage of using PCMMU data is that it incorporates some data not available to the Orbiter's General Purpose Computers (GPCs). A drawback of the Portable Grid System Computer (PGSC) laptop is that it can not be used during ascent and descent. The laptops have to be secured in the lockers for these phases of flight. While in use, the laptop requires long connector cables which restrict space and crew movements in the Orbiter's cockpit. A block diagram of the basic setup is shown in Fig. 4.1.

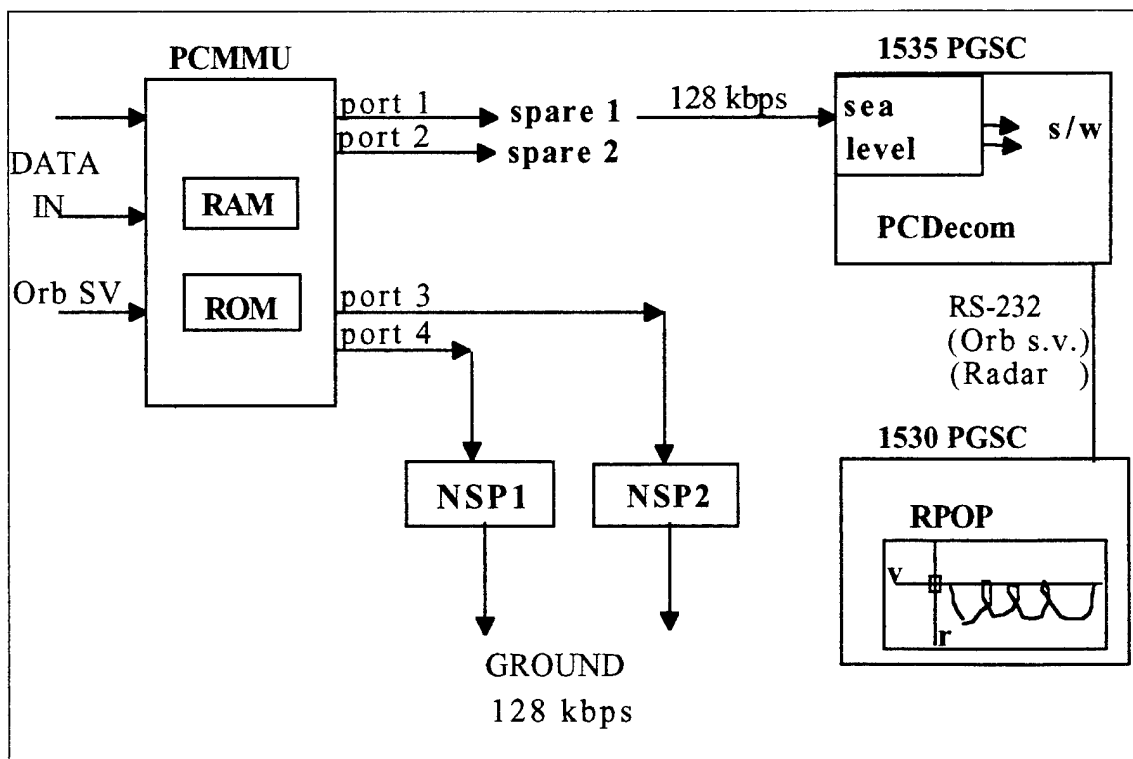


Figure 4.1. PGSC Experiment block diagram.

The source for the 128 Kbyte data link information comes from the PCMMU. This data stream is used to down-link and up-link all telemetry information from the Shuttle to Mission Command Center (MCC). The PCMMU has four ports, two are used by MCC and two are spares, which put out identical information. The Graphic Retrieval and Information Display (GRID) 1535 laptop computer, linked through a 128 Kbyte data link cable, acts as the interface between the PCMMU and the GRID 1530 PGSC. The GRID 1535 contains an RS-422 Sea Level card which provides an asynchronous serial Input/Output (I/O) and the PC Decommutator (PCDecom) software package which decommutates and selects data for output. Data from the GRID 1535 to the GRID 1530 is transmitted via the RS-232 communication port. These GRID laptop computers will soon be replaced with an IBM Thinkpad 700 series laptop. [Ref. 10]

Data from the GRID 1535 is used by the NPS software program Rendezvous/Prox Ops Program (RPOP), which resides in the GRID 1530 laptop, to automate rendezvous procedures. The NPS RPOP display, shown in Fig. 4.2, can be used to view relative motion between the target, which is stationary, and the chase vehicle. By adjusting flight data, predicted results of upcoming maneuvers are depicted. Detailed information on the NPS software and the experiment can be found in Ref. 10. The NPS software has been flown on several Shuttle missions starting with STS-51 and have contributed to the use of real-time data analysis to increase the crew's situational awareness. The RPOP display is a direct result of a certified rendezvous software, Payload Bay (PLBAY), currently used by NASA on the ground. The PLBAY program is not automated and requires numerous inputs from the user. There are indications that various features of the NPS software will be incorporated into a certified version of the NASA code in the future. [Ref. 10]

#### **D. PROPOSED INCORPORATION OF MEDS**

The RPOP display is a good example of an advanced Orbiter display preferred by the crew during the rendezvous phase. Once the MEDS is incorporated, the RPOP display can be depicted on the Multifunction Display Unit (MDU) vice a laptop computer.

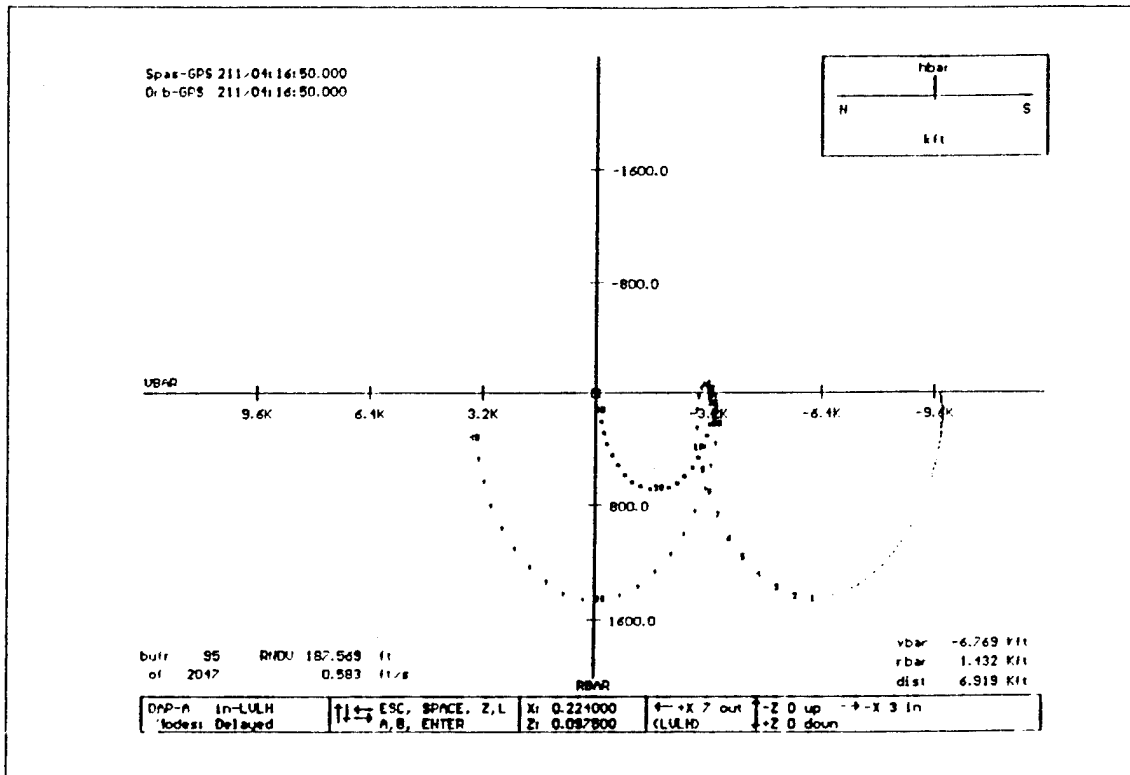


Figure 4.2. RPOP Sample R-bar/V-bar plot. (from Ref. [10])

There are three options of incorporating the MEDS into the Shuttle, each with its advantages and disadvantages.

### 1. Altering the Flight Software

The IDP gets information directly from the GPC via the data bus. Transferring additional data to the IDP requires altering the orbiter's flight software. The advantage of this method is that there are no additional hardware or changes necessary to the MEDS. The major disadvantages of this method are high costs and time required to implement and test any changes in critical flight software. The software validation and certification process takes a minimum of one year to complete and NASA management is strongly against the idea of altering the flight software. The other disadvantage is that not all of the Orbiter's information are available to the GPC. Unlike the GPC, the PCMMU gets all Orbiter information.

## 2. PCMMU Link to the Primary Side of the IDP

The PCMMU can be linked to the primary side of the IDP if a RS-422 Sea Level card is added to the spare slot in the IDP. Shown in Fig. 4.3 is the block diagram of how this can be implemented. This spare slot is shown as "growth SRU" on the MEDS DX Backplane, in Fig 3.4 above. The RS-422 Sea Level card, which performs the same function as the one described in the above experiment, can be acquired from Honeywell. This method gives the IDP all data available from the GPC plus the PCMMU. However, it still has disadvantages such as costs, altering the flight software and certification.

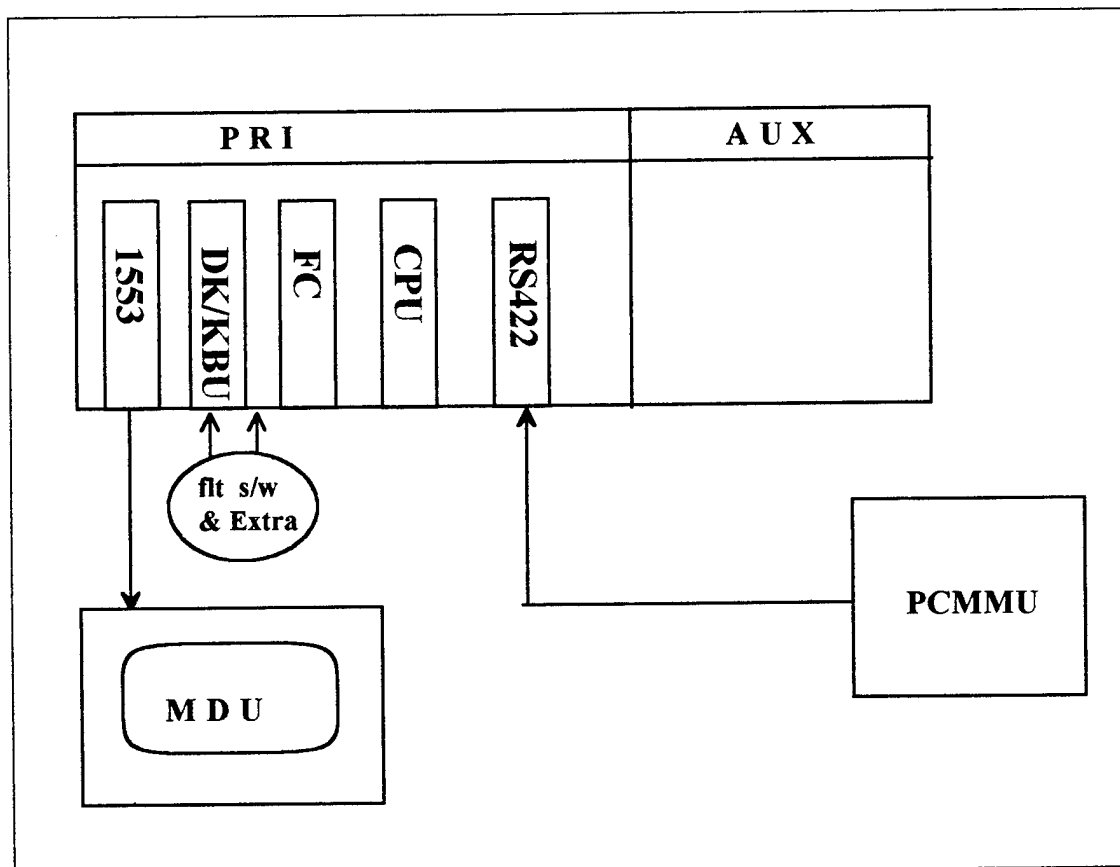


Figure 4.3. PCMMU to Primary Side of IDP.

### 3. PCMMU Link to the Auxiliary Side of the IDP

A more feasible approach than the two methods described in section 1 and 2 is to link the PCMMU to the spare slots of the AUX DX Backplane of the IDP, shown in Fig 4.4 below. This entails adding the following hardware to the IDP: RS-422 Sea Level card; a CPU; and a TARGAT video card. The MDU also requires a video card for this method. Without connecting the bridge, the data can be completely isolated from the MEDS DX Backplane of the IDP. This method does not involve altering the flight software and opens up a wide range of significant information that can be displayed with the MEDS. Certified software would be required if there are future intentions of making data from the PCMMU flight critical data.

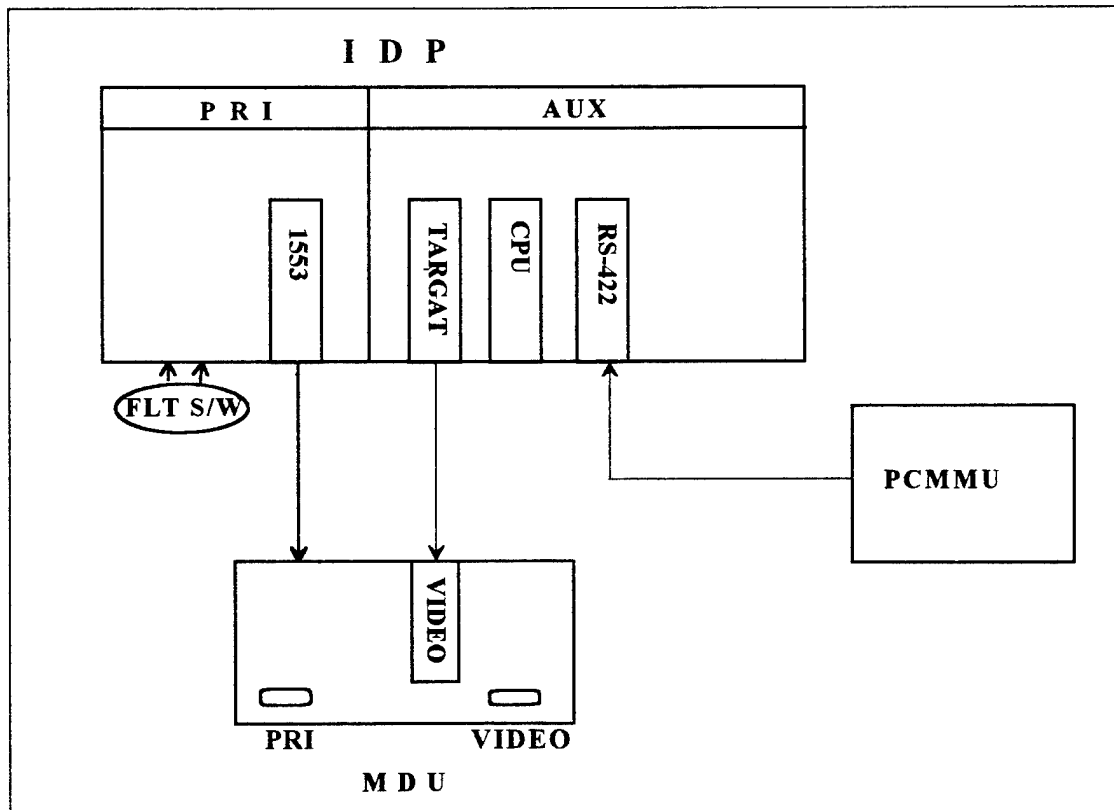


Figure 4.4. PCMMU to Auxiliary Side of IDP.

## E. ASCENT ABORTS

Before developing the proposed ascent/descent advanced orbiter display, a better understanding of the various inflight abort types and procedures are required. There are two types of events that requires the Shuttle to perform an inflight abort: performance and system failures. Our concern here is with the performance failure; the time when a Space Shuttle Main Engine (SSME) loses thrust or simply fails to function. The two types of ascent abort modes are: intact aborts and contingency aborts. The intact aborts provide a safe return of the orbiter to a planned landing site, and the contingency aborts follow more severe failures which usually result in a crew bailout.

Some of the intact aborts include an abort to orbit (ATO), an abort once around (AOA), a transoceanic abort landing (TAL), and a return to launch site (RTLS). An ATO occurs late in the ascent phase when the orbiter comes close to achieving a normal orbit, but simply goes to a perfectly safe lower orbit. An AOA is used when the ATO cannot be achieved. The orbiter is placed into a sub-orbital trajectory leading to a landing after one revolution of the Earth. If this can not be achieved, the TAL is used. Figure 4.5 shows a TAL versus nominal ascent profile. This results in landing on a runway in Europe or Africa. In the case that one of the SSMEs fails after lift-off and before a TAL can be achieved, a RTLS is performed. Figure 4.6 shows a typical RTLS profile. During powered flight, the crew receive present abort capability calls from the MCC that are determined by a computer program called the Abort Region Determinator (ARD). Some MCC calls are given in Ref. 11. The ARD takes into account real time data to predict real time mode boundaries. [Ref. 7]

There are numerous abort mode boundaries and each is time dependent and flight-specific. The mass properties, environmental modeling, and performance characteristics change significantly with time. The boundaries are different with higher inclination flights than lower inclination flights. Most of the following boundaries are based on the orbiter's state vector and available thrust; two-engine TAL, negative return,



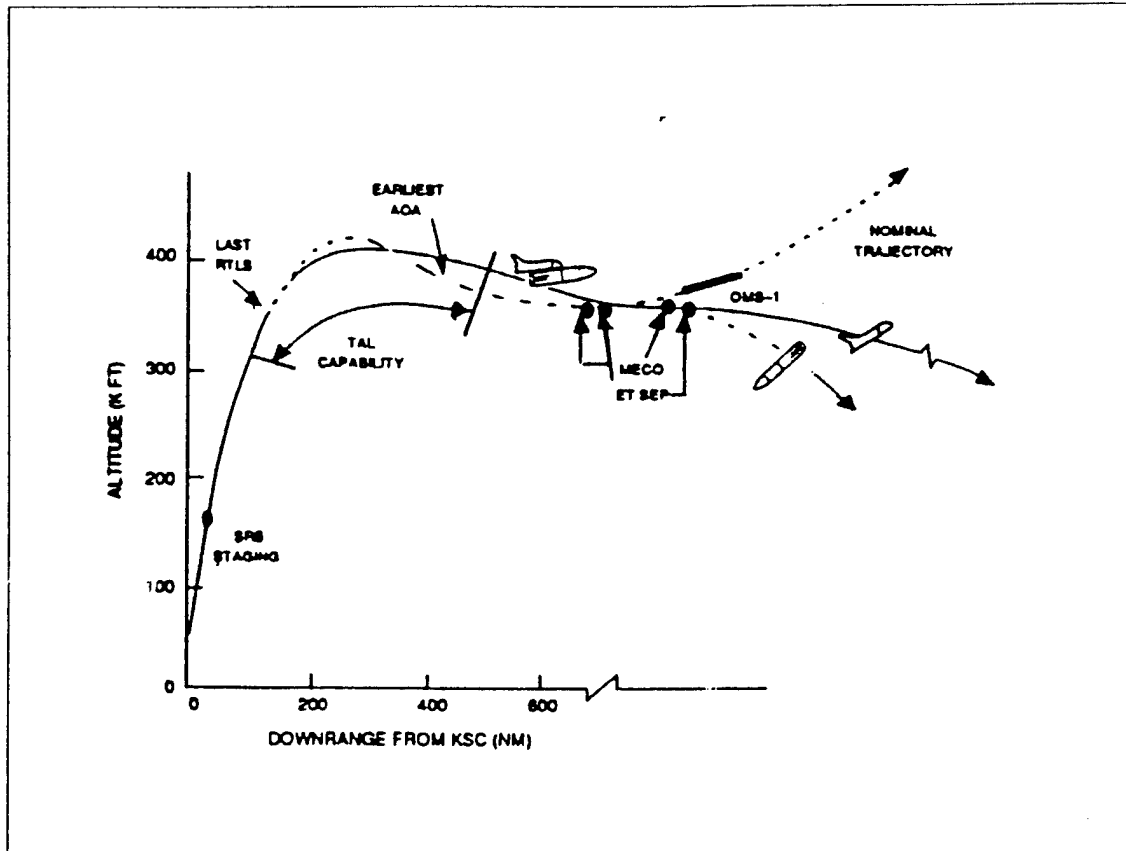


Figure 4.5. TAL versus Nominal Ascent profile. (From Ref. [7])

press to ATO, press to MECO, DROOP (109), single engine (SE) TAL (104), SE press, last pre-MECO TAL, and last TAL. [Ref. 7]

## F. ASCENT/DESCENT ADVANCED ORBITER DISPLAYS

The purpose of the proposed display is to increase the flight crew situational awareness, simply by displaying the downrange and crossrange capabilities of the Orbiter. Presently, the abort procedure during the loss of an SSME engine takes approximately four to five minutes to be identified and resolved. The proposed Orbiter's display will give the crew a quick reference as to the type of abort modes available. The display by no means replaces or reduces the reliance on ground control, but is used in conjunction with MCC. The next chapter of this thesis will address the way in which real time data can be processed by MEDS and displayed on the MDUs. The displays in Fig. 4.7 and Fig. 4.8

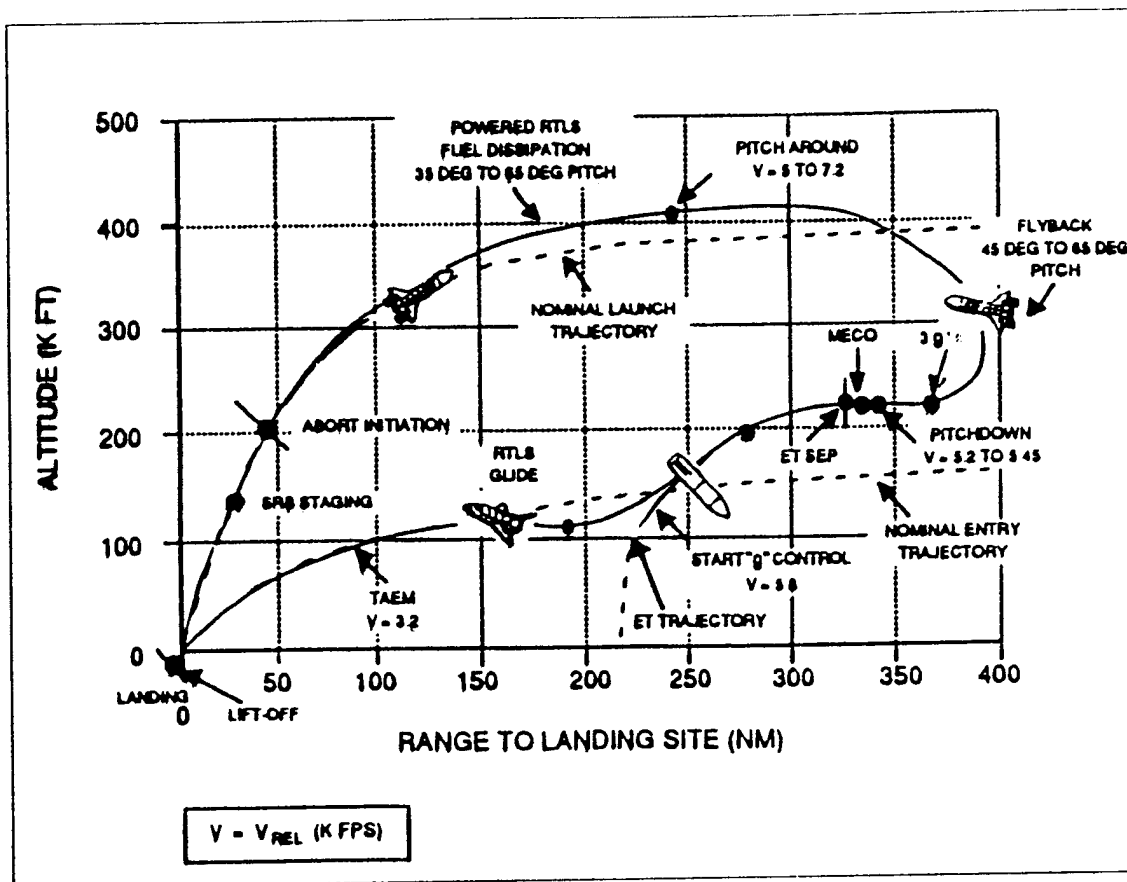


Figure 4.6. RTLS profile. (From Ref. [7])

are not generated by actual flight data information, but simply static pictures used for illustration. The two displays below are depicted at different times to show the dynamic of the range capability.

The display in Fig. 4.7 shows a real time landing footprint with predicted abort boundaries color coded for the case of one engine out (EO), two EO and three EO. All information displayed uses real time onboard state vector information. It is important to note that the display does not flash at any time and the geographical map moves with time, not the abort boundaries. The EO boundaries will change or disappear with time. As an example, if a 2 EO occurs, the 1 EO green boundary will not be displayed and so on. The Mission Elapsed Time (MET) box displays the time from lift-off. During this first one minute and forty-five seconds' period, the shuttle is on a vertical climb and increasing

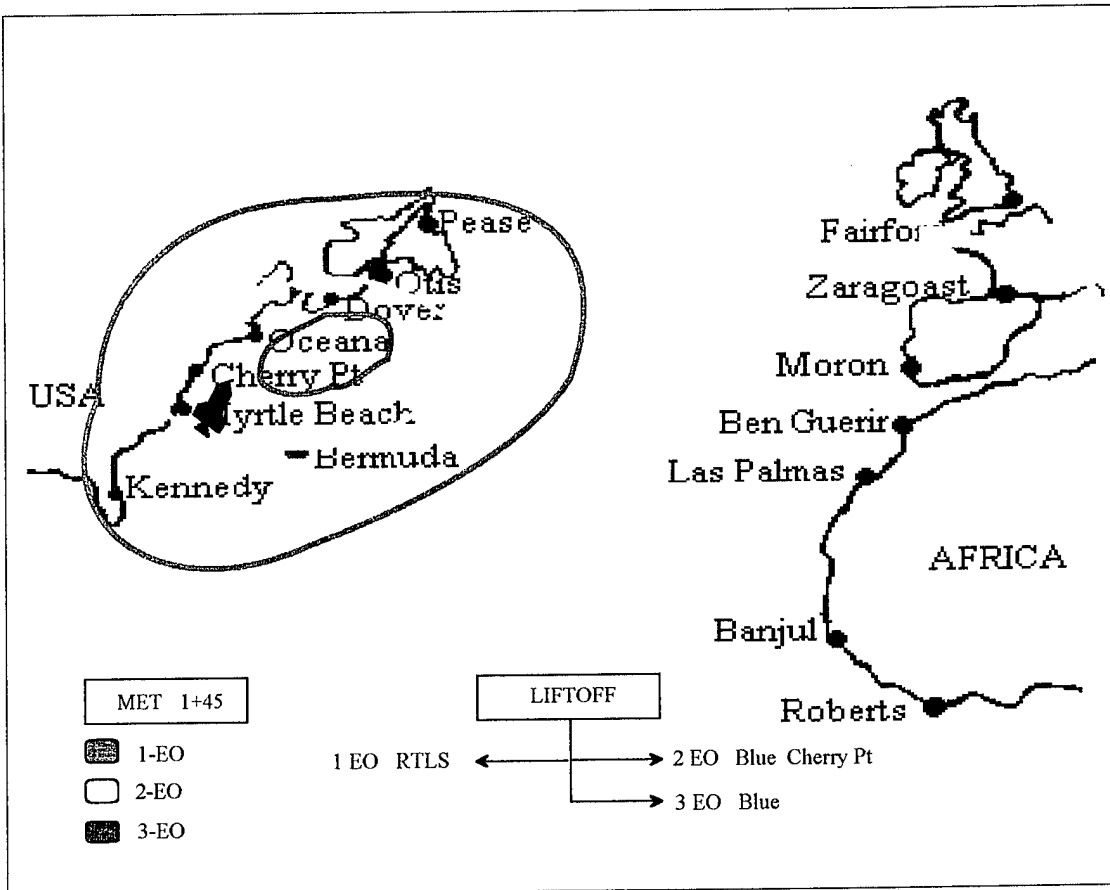


Figure 4.7. Proposed Ascent Displayed at MET 1+45.

velocity rapidly. The current status box (LIFTOFF) emulates MCC calls, as described in section A above. The status box changes with time based on onboard state vector information and predetermined flight data. The decision tree below the status box gives the nominal abort landing sites or procedures for all three EO cases. Note that the color code used by the decision tree is not related to the color coded boundary regions. The display can be magnified when in proximity of a landing site for making the bailout decision in tight situations. In most 1 EO cases, the Shuttle will continue to press on. Although bailout zones are not explicitly depicted, they are the same as EO zones that do not encompass a landing site.

Figure 4.8 depicts the same scenario as Fig. 4.7, except at MET equals five minutes and thirty seconds. Note that as the Orbiter velocity is increased the boundary

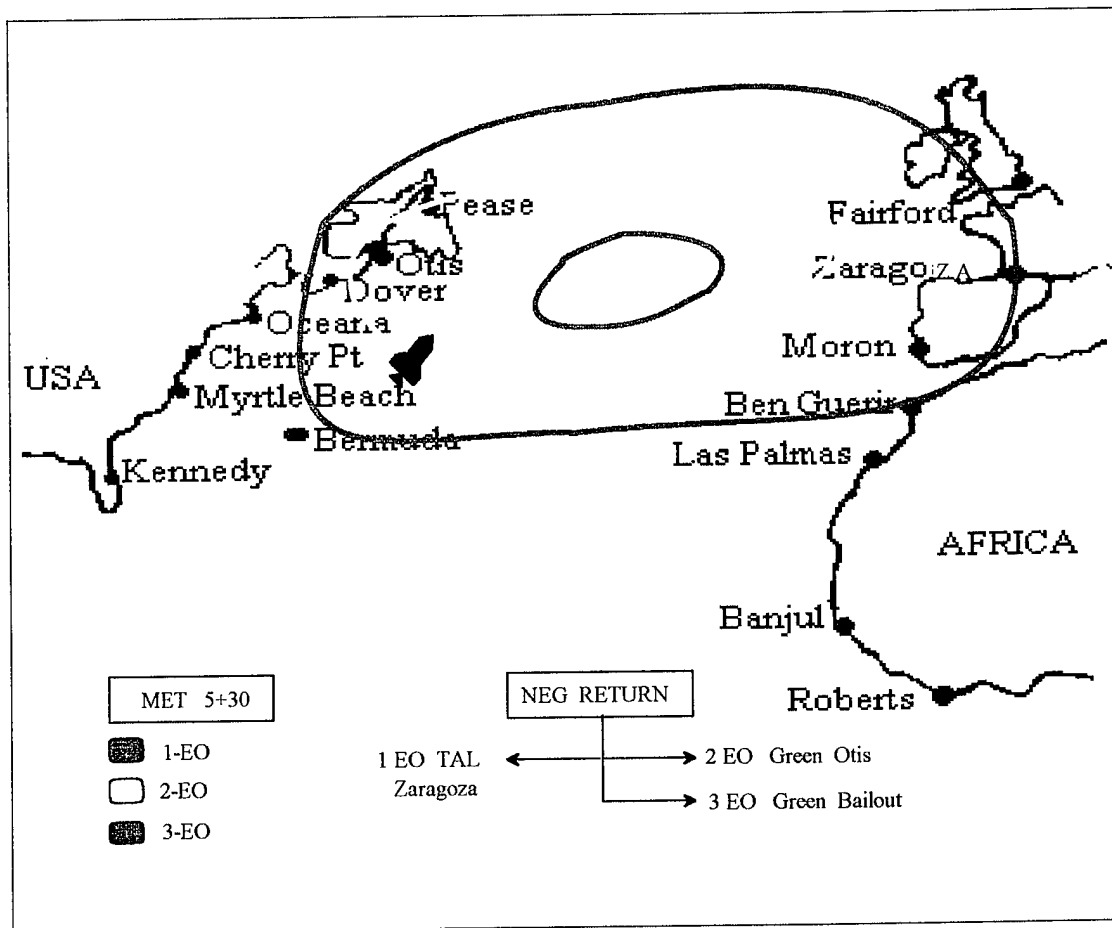


Figure 4.8. Proposed Ascent Displayed at MET 5+30.

gets elongated. There is an overlapping period just before NEG Return where the orbiter has both TAL and RTLS capability. The decision tree can display Black zones as "3 EO Black" when in proximity to the selected landing site.



## V. DOWNRANGE ABORT EVALUATOR (DAE)

The abort regions shown in Fig. 4.7 and 4.8 can be determined by integrating the equations of motion for a rigid body flying through the atmosphere. A Matlab program was developed to show the downrange and crossrange capabilities based on a given Orbiter state vector. The resultant output for a specific case is then compared with NASA's Downrange Abort Evaluator (DAE) program output.

### A. EQUATIONS OF MOTION

The trajectory of a vehicle can be determined by applying Newton's law of motion,  $F=ma$ . The dynamic (forces) and kinematic (velocities) equations are given in Ref. 12. Some of the equations are modified to make them consistent with the reference frame used. Rewriting Newton's law of motions gives,  $A=F_l + F_d + F_{th} + G$ . Figure 5.1 illustrates forces that are acting on a vehicle as it is flying through the atmosphere.

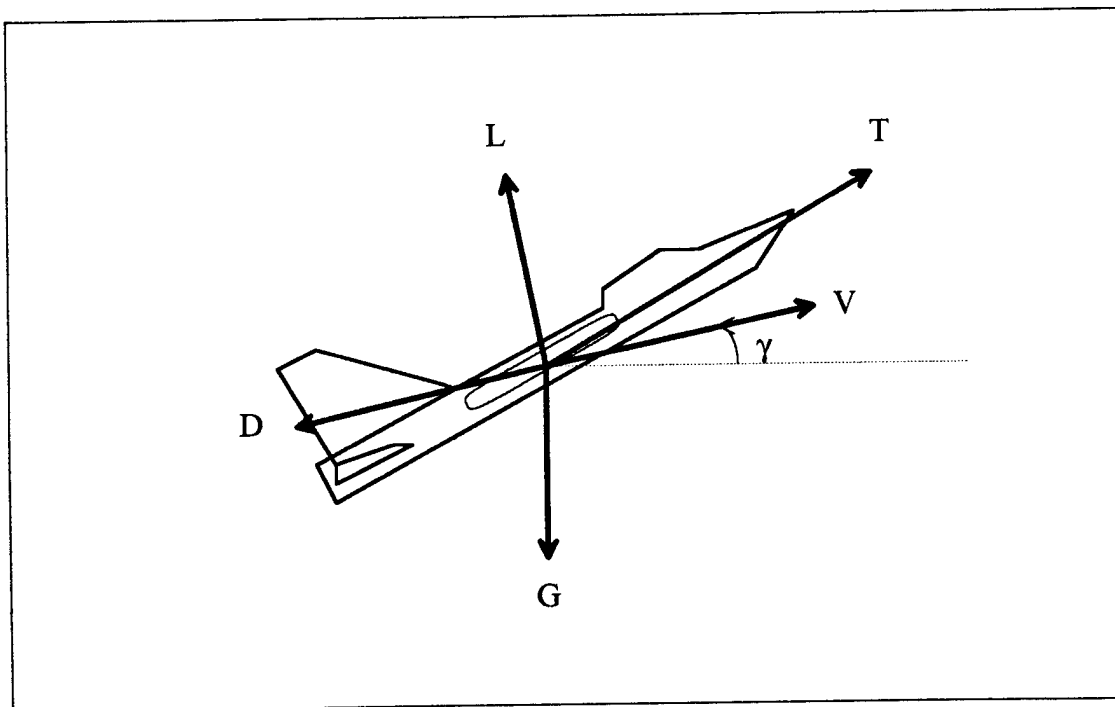


Figure 5.1. Vehicle Forces During Atmospheric Interaction.

## 1. Reference Frame

A geocentric latitude-longitude reference frame ( $R, \lambda_{TP}, \Lambda$ ) is shown in Fig. 5.2. Where  $R$  is the geocentric radius from the center of the Earth to the vehicle.  $\lambda_{TP}$  is the inertial geocentric longitude of the vehicle; measured in equatorial plane from  $X_I$  to the vehicle at  $P$ .  $\Lambda$  is the geocentric latitude of the vehicle. A vehicle coordinates frame is shown in Fig. 5.3.

## 2. Kinematics

The kinematic equations of the vehicle are based on the position of the vehicle and the linear velocity. By using the law of Coriolis, an expression for the acceleration of the vehicle is given by:

$$A = (R'' - R \Lambda'^2 - R \lambda_{TP}'^2 \cos^2 \Lambda) I_r + [d(R^2 \lambda_{TP}' \cos^2 \Lambda)/dt * 1/R \cos \Lambda] I_\lambda + (R \Lambda'' + 2 R' \Lambda' + R \lambda_{TP}'^2 \cos \Lambda \sin \Lambda) I_\Lambda$$

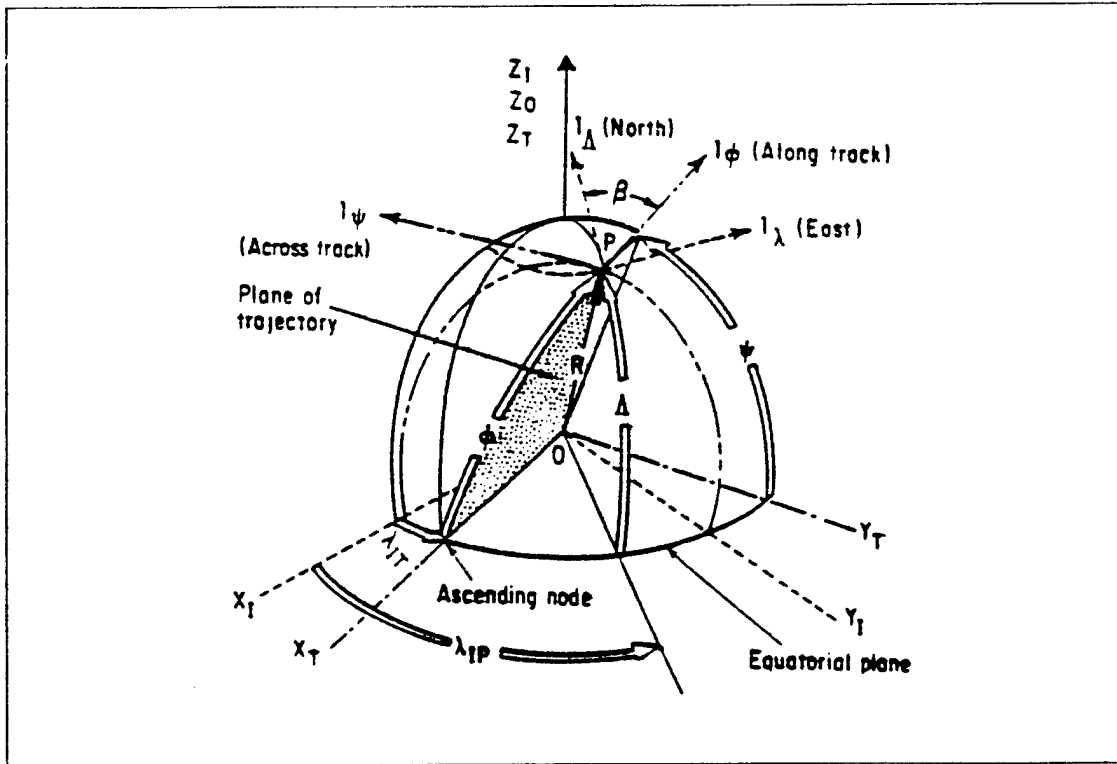


Figure 5.2. Geocentric Latitude-Longitude Reference Frame. (From Ref. [12])

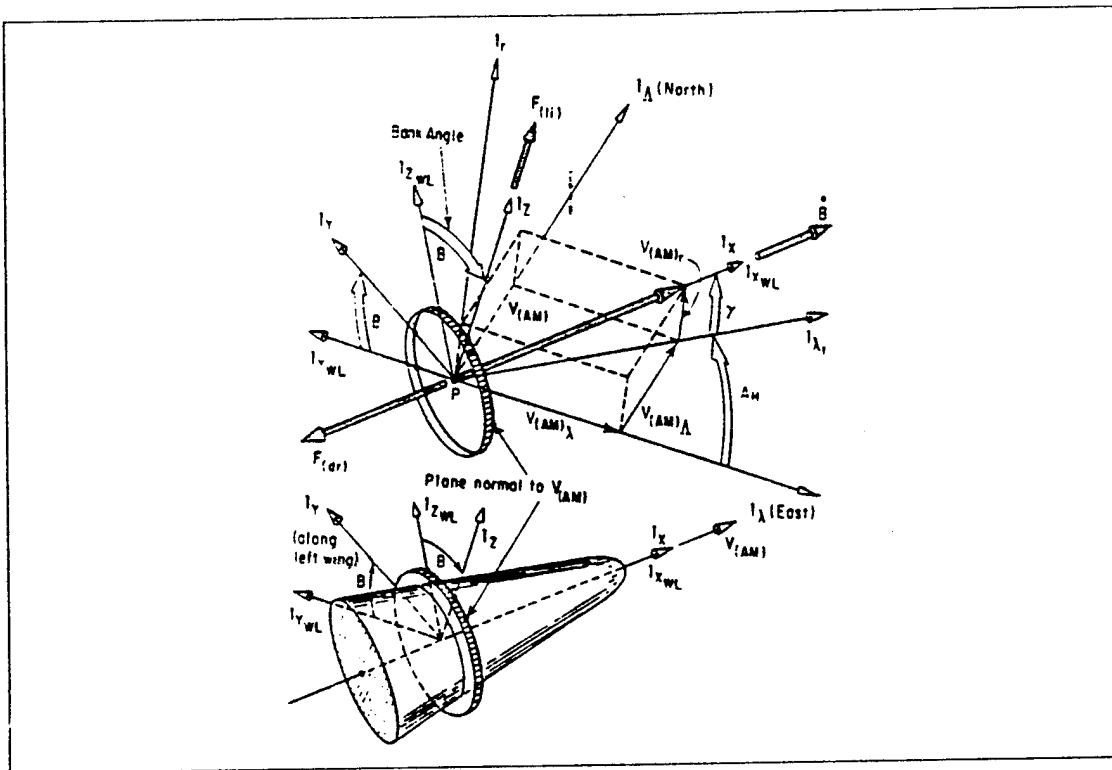


Figure 5.3. Vehicle Coordinate Frame. (From Ref. [12])

### 3. Gravitational Force

The gravitational force equation takes into account the oblateness of the Earth and the distance from the Earth's center. The gravitational component is given as follow:

$$G_r = -G_{sp} + 3 v G_{sp} (R_{eq}/R)^2 (1 - 3 \cos 2 \Lambda)$$

$$G_\lambda = 0$$

$$G_\Lambda = -6 v G_{sp} (R_{eq}/R)^2 \sin 2 \Lambda$$

Where  $G_{sp}$  is the spherical gravitational mass of attraction, and  $R_{eq}$  is the Radius of the Earth at the equator.

### 4. Drag Force

Drag forces are produced as the vehicle moves through the sensible atmosphere. It is highly dependent on the atmospheric density, surface area of the vehicle, and vehicle



velocity. The atmospheric model, given in Ref. 13, is based on a two-parameter atmosphere model given as,

$$\rho = \rho_o \exp (- h / H)$$

Where  $h$  is the altitude and  $H$  is the atmospheric scale height. Modeling the 1976 U.S. Standard Atmosphere, a value of 6.7km is used for  $H$  and a value of 1.752 kg/m<sup>3</sup> is used for  $\rho_o$ . These values are adjustable to give a better fit over the altitude range of interest. The drag force components are given as follow:

$$F_r = - \rho C_d S V_{am} R' / 2 M$$

$$F_\lambda = - \rho C_d S V_{am} R \cos \Lambda (\lambda_{ip}' - W_{io}) / 2 M$$

$$F_\Lambda = - \rho C_d S V_{am} R \Lambda' / 2 M$$

Where  $\rho$  is the atmospheric density,  $C_d$  is the coefficient of drag,  $S$  is the vehicle surface area,  $V_{am}$  is the atmospheric velocity, and  $M$  is the mass of the vehicle.

## 5. Lift Force

Lift forces are also produced as the vehicle moves through the atmosphere. Lift force is dependent on the atmospheric density, surface area of the vehicle, vehicle velocity and its configuration. The lift force components are given as follow:

$$F_r = \rho C_l S / 2 M ( (V_{am_\lambda})^2 + (V_{am_\Lambda})^2 )^{1/2} V_{am} \cos B$$

$$F_\lambda = \rho C_l S V_{am} / 2 M [ V_{am} V_{am_\Lambda} \sin B - R' V_{am_\lambda} \cos B / ( (V_{am_\lambda})^2 + (V_{am_\Lambda})^2 )^{1/2} ]$$

$$F_\Lambda = - \rho C_l S V_{am} / 2 M [ V_{am} V_{am_\lambda} \sin B + R' V_{am_\Lambda} \cos B / ( (V_{am_\lambda})^2 + (V_{am_\Lambda})^2 )^{1/2} ]$$

Where  $C_l$  is the coefficient of lift, and  $B$  is the bank angle.

## 6. Thrust Force

Thrust forces for the Space Shuttle during ascent are available until the External Tank separates. The primary thrust used for maneuver comes from the three SSMEs. The thrust force components are given as follow:

$$F_r = - \Gamma V_e / M [ \cos A_e \cos A_d \sin \gamma + \sin A_d \cos \gamma \sin B + \sin A_e \cos A_d \cos \gamma \cos B ]$$

$$F_\lambda = - \Gamma V_e / M [ \cos A_e \cos A_d \cos \gamma \cos A_h - \sin A_d \sin A_h \cos B ]$$

$$\begin{aligned}
& - \sin A_d \cos \gamma \cos A_h \sin B + \sin A_e \cos A_d \sin A_h \sin B \\
& - \sin A_e \cos A_d \sin \gamma \cos A_h \cos B ]
\end{aligned}$$

$$\begin{aligned}
F_A = - \Gamma V_e / M [ & \cos A_e \cos A_d \cos \gamma \sin A_h + \sin A_d \cos A_h \cos B \\
& - \sin A_d \sin \gamma \sin A_h \sin B - \sin A_e \cos A_d \cos A_h \sin B \\
& - \sin A_e \cos A_d \sin \gamma \sin A_h \cos B ]
\end{aligned}$$

See Appendix B for definition of all symbols.

## B. MATLAB PROGRAM

The equations of motion given above can be written in state space form, which is an integratable format, and integrated by using a second and third order integrator. This is accomplished by using Matlab with Simulink, version 4.0, developed by the Mathworks, Inc.

The programs SHUTTLE and INIT, see Appendix B, are a Matlab function file and script file, respectively. The program predicts the impact point of the orbiter by numerically integrating the trajectory, taking into account vehicle aerodynamics and gravitational affects. An initial Orbiter state vector is required as the input for both programs. The output program INIT gives the geocentric latitude and inertial geocentric longitude of the impact point. These values are then converted from radians to degrees and from inertial geocentric longitude to geocentric longitude. By varying the initial conditions, data from each trial run is entered into a spreadsheet and plotted. The resultant plot displays the landing footprint that represents the orbiter's maneuvering capabilities.

### 1. Space Shuttle 3 EO Case Study

A specific case of three engines out is analyzed for the Space Shuttle. In this case, the decision has been made to perform a TAL abort and the ET has been separated. At this point in the trajectory, no thrust is available to the Shuttle. It becomes a glider and has only one chance for a controlled landing.

To effectively compare the Matlab result with NASA's result, the same initial conditions must be used. However, not all the initial condition parameters from the NASA code can be put into the form used by the Matlab code. Therefore, the data are interpolated and expressed in a format usable to the Matlab code. All efforts were made to simulate these conditions as closely as possible.

There are many Orbiter parameters (e.g., B, AOA) that can be varied; the limiting case of each parameter is used to predict the output. All parameters were kept within the physical limitations of the Space Shuttle. The maximum bank angle used was  $\pm 50$  degrees. The angle of attack varied from 0-42 degrees depending on the altitude. The scale height (H) and initial density (h) were varied slightly from the 1976 U.S. Standard Atmospheric model to fit the altitude range from 0 to 360,000 feet. The coefficient of lift and drag were also varied to simulated different configurations. A constant frontal surface area and mass were used in this case due to the limitations of the code. The Orbiter's impact point is determined when the vehicle's altitude is approximately equal to zero (within the model), due to the integration method used.

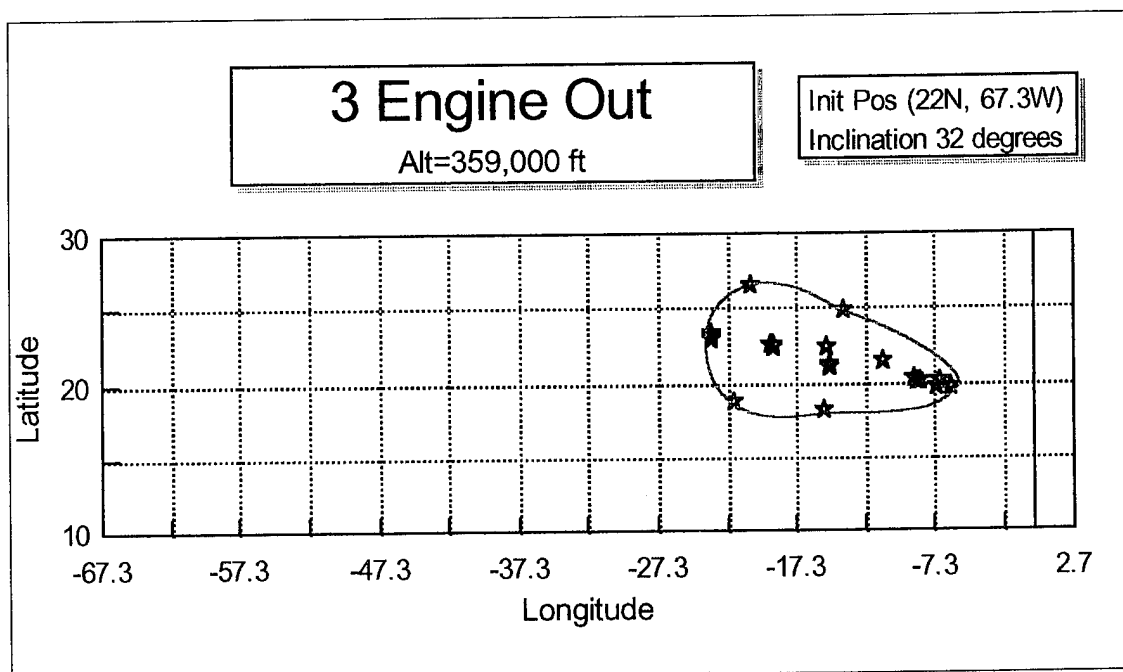


Figure 5.4. Matlab Result For 3 EO case.

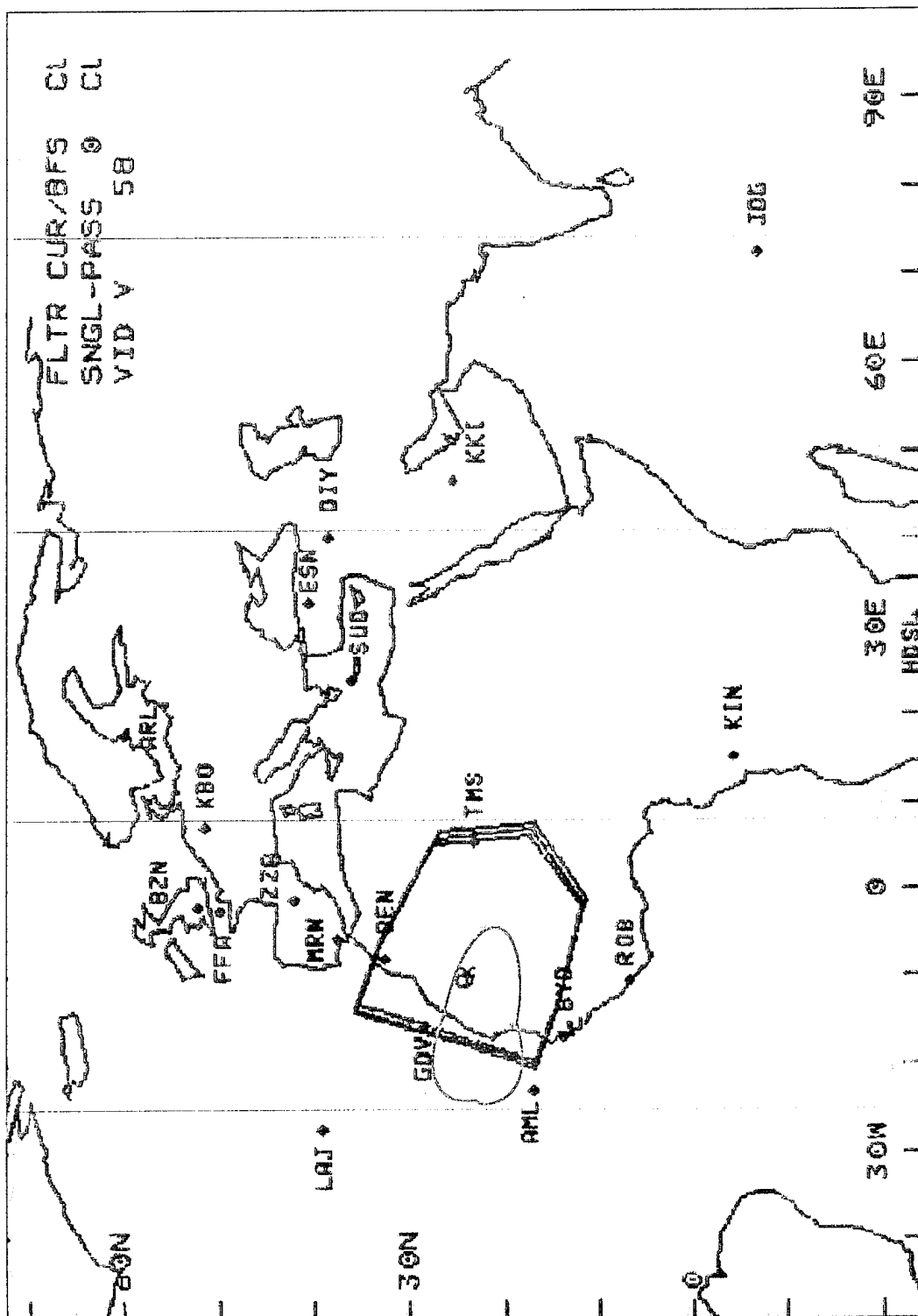


Figure 5.5. Comparison of Matlab vs. NASA DAE Code.

The initial position was at 22N Latitude and 67.3W, the initial altitude was at 359,000 ft and the relative velocity is 22,840 ft/s. The result, given in Fig. 5.4, shows that the maximum downrange longitude is 5W, the minimum is 24W and the crossrange varies from 18N to 27N latitude. The individual points are specific case outputs and the boundary connecting the points is what the boundary would look like if all cases were taken into account.

### **C. DATA COMPARISON**

The result of the Matlab code is overlaid on the NASA DAE output as shown in Fig. 5.5. To get a better understanding of the differences in the results, a more in-depth analysis of the DAE code is presented and possible differences are discussed.

#### **1. Downrange Abort Evaluator (DAE)**

The Downrange Abort Evaluator predicts the impact point by propagating the input state vector to a threshold altitude, from which point the range to impact is computed by a table lookup of energy versus range. The propagation is followed by a numerical integration of the trajectory, taking into account a first order lag flight control system, a simplified entry guidance system, vehicle aerodynamics and a central gravitational term. This integration is continued until the integrated trajectory converges to a built-in drag-velocity profile, at which point the range to impact can be computed analytically. A "canned" drag-velocity profile is used to compute the distance the orbiter would fly should that profile be followed. A landing footprint is then generated based on the predicted impact point. The tables used were based on a history of simulation runs conducted in the flight simulator at the Johnson Space Center.

#### **2. Possible Output Differences**

The data output received from the DAE were based on a simulation that takes into account a dynamically controlled orbiter and its onboard guidance algorithm. The Matlab

model uses only constant vehicle parameters which correlates to a static configuration throughout the vehicle's trajectory.

One major difference is the use of a simplified entry guidance system by the DAE. Different drag profiles were used at different phases of flight by the DAE vice a single constant drag profile used by the Matlab code. The DAE's range predictions were based on solutions to the equations of motion for specified Orbiter drag profiles, which are a function of the Orbiter's velocity. Different Orbiter drag profiles were used for the temperature control phase, the equilibrium glide phase, the constant drag phase and the transition phase. One particular example is that the scale height is varied throughout the vehicle's trajectory vice the constant scale height used by the Matlab program.

The routine to determine the impact point used by the Matlab code is not precise. It determines whether the integrated altitude is within a range of the reference altitude of zero. However, this is not a significant error since it only causes a 1-2 degree error in the latitude or longitude of the output.

The DAE also uses geodetic latitude and longitude vice geocentric latitude and longitude as used by the Matlab program. However, this is not a significant difference due to the very small eccentricity of the Earth's oblateness. The error caused by this is less than one degree in latitude or longitude. In spite of these differences, the two landing footprints are fairly close.



## **VI. CONCLUSIONS**

The National Aeronautics and Space Administration (NASA) recognized that there was a need to upgrade the Space Shuttle's cockpit display subsystem. The result is a state-of-the-art Multifunction Electronic Display Subsystem (MEDS) which uses color Active Matrix Liquid Crystal Displays (AMLCDs). Initially, the MEDS display will graphically mimic the current cockpit display instruments to minimize crew training impacts. However, with the MEDS' intrinsic growth provisions, the advanced capabilities of MEDS will be invoked. In order to optimize the Orbiter's cockpit, new advanced orbiter display formats need to be developed. The analysis of the Orbiter's state vectors demonstrated that three methods of implementing MEDS allowed for real-time graphical displays to be depicted. Optimization of the Orbiter's cockpit using the MEDS allowed two displays, currently only used on the ground, to be displayed onboard the Orbiter. The two displays are: Rendezvous Proximity/Ops Program (RPOP) display; and the proposed ascent/entry display. The processing capability of the MEDS was emulated by using a personal computer to demonstrate that prototype advanced orbiter display formats can be generated.

### **A. OPTIMAL MEDS IMPLEMENTATION METHODS**

A great deal of innovative design went into the development of the MEDS. Its similarity with a desktop computer allowed room for future improvements and its modularity allowed easy in-flight maintenance. By connecting the Pulse Code Modulator Master Unit (PCMMU) data to the MEDS, real-time data are available for situational awareness to assist the flight crew during critical phases of flight. The optimal method is achieved by linking the PCMMU to the AUX side of the Integrated Display Processor (IDP). This method is totally isolated from the primary side of the IDP and does not involve altering the primary flight software. NASA is actively pursuing various means of full utilization of this real-time data for other Shuttle's subsystems. The opportunities for future research and development of the MEDS are significant.



## **A. FINAL PROPOSED DESIGN**

As a direct result of crew preference, a design for an advanced orbiter display was developed. The result is a display showing predicted Orbiter impact landing footprints, for three different cases of one, two and three engines out, during the ascent phase of flight. These graphical displays enhance the crew's situational awareness and together with ground data inputs could increase safety of flight. Many more display designs are needed for this phase and other phases of the Shuttle's mission.

## **B. RESULTS OF MATLAB VS. NASA'S DAE**

A Matlab program, developed and processed on a 486DX personal computer, demonstrated that these real-time abort regions can easily be incorporated into the MEDS. Results from the Matlab code were compared with NASA Downrange Abort Evaluator (DAE) code for a specific case of three engines out. The two regions were relatively close despite differences in control and guidance algorithms. Much improvement can be done with the Matlab program in control and guidance to improve its accuracy. It is not necessary to use Matlab as a program language; any high order language such as ADA or C++ or FORTRAN will suffice. This program is a stepping stone to a critical and powerful concept.

## **C. RECOMMENDATIONS**

It is the hope of the author that others will continue to develop new advanced orbiter displays, develop alternative methods of implementing the MEDS and to make improvements to the Matlab (or alternate) program. Another area of the MEDS that requires development is the display application software for the proposed and new advanced orbiter displays.

## LIST OF REFERENCES

1. Spitzer, C. R., Digital Avionics System, McGraw-Hill Book Company, Inc., 1993.
2. Abbott, T. S., Task-Oriented Display Design, Society of Automotive Engineers, Inc., 1989.
3. Ratliff, J. E., Multifunction Electronic Display Subsystem Program Overview, Johnson Space Center, Houston, Texas, Aug 10, 1994.
4. Hanaway, J. F., Moorehead R.W., Space Shuttle Avionics System, U.S. Government Printing Office, Washington, DC, 1989.
5. Agrawal, B. N., Design of Geosynchronous Spacecraft, Prentice-Hall, Inc., 1986.
6. Honeywell Inc., Multifunction Electronic Display Subsystem, Critical Design Review, 1994.
7. Shuttle Crew Operations Manual (SCOM 1.2), Nov 92.
8. MEDS System Segment Specification, SSD92D0643B, Revision B, Rockwell International, Space System Division, Jan 19, 1994.
9. Rominger, Kent, CB, Advanced Orbiter Displays, NASA, Johnson Space Center, Houston, Texas, Aug 10, 1994.
10. Barker, L. A., Thesis, NPS State Vector Analysis and Relative motion Plotting Software for STS-51, Monterey, California, Mar 1994.
11. Precourt, C., CB, Mastracchio, R., CA4, Contingency Aborts OI-21, NASA, Johnson Space Center, June 1992.
12. Duncan, R. C., Dynamics of Atmospheric Entry, McGraw-Hill Book Company, Inc., 1962.
13. Regan, F. J., Anandakrishnan, S. M., Dynamics of Atmospheric Re-Entry, American Institute of Aeronautics and Astronautics, Inc., 1993.
14. Thomsen, S. V., Hancock W. R., High-Performance, AMLCD-Based "Smart" Display for The Space Shuttle Glass Cockpit, 13th Digital Avionics Systems Conference, Phoenix, Arizona, Honeywell Inc., Oct 31, 1994.



## APPENDIX A. MEDS HARDWARE SPECIFICATIONS

Design Parameter	MDU Performance (Ref. 14)	
CPU throughput	20 MIPS/7.4 MFLOPS	
R3081E	6.0 MIPS	
34020		
Display pipeline BW	478M bits/s	
VG drawing rate	65.5K vector in./s 32.8K arc in./s 3.4M points/s	
Anti-aliasing/halo imaging filter BW	3.50 BOPS	
System memory	1.5Mb SRAM	
R3081E	1.0Mb EEPROM	
34020	512Kb SRAM	
	1.4Mb VRAM	
1553B interface	128K SRAM	
Envelope	8 in. H x 8.75 in. W x 8.75in. D	
Weight	17.2 lb	
Cooling	Forced air (0.41 lb/hr/W)	
Operating power	Typical	Worst Case
Graphics at 100 fL	80 W	91 W
Graphics at lamp EOL	92 W	103 W
Video at 100 fL	84 W	95 W
Video at lamp EOL	95 W	106 W
Environmental		
Vibration	7.85 g rms, each axis	
Shock	15g MIL-STD-810C	
Humidity	810C (507.1); Proc IV	
Salt-fog	810C (509.1); Proc I	
EMI/EMC	MIL-STD-461/462	
Temperature	-30 to +65 degree C	
Lightning	MIL-B5087B	
Acceleration	+/- 5g, each axis	
Acoustic exposure	810C (512.2); Proc I	
BIT coverage	98% (initiated) 83% (periodic)	

Display Parameter	MDU Performance (Ref. 14)
Active viewing area	6.71 x 6.71 in.
Color dot resolution	172 dot/in.
LCD dot matrix	1152 x 1152
Pixel arrangement	RGB triad
Viewing angles	Horizontal: +/- 60 degrees Vertical: -10 deg/+45 deg
Contrast ratio (<1 fc) ERP H(+/-20):V(0/+20) H(+/-45):V(-10/+30) H(+/-60):V(-10/+45)	>90:1 >65:1 >45:1 >15:1
Contrast ratio (high ambient)	>6:1 (all angles)
Display leakage	<3.5 fL (all angles)
Specular reflectance	1.00% at 30 deg
Diffuse reflectance	0.06% at 30 deg
Luminance uniformity	Red: 11.5% Grn: 12.9% Blu: 16% Wht: 16% Blk: 18%
Color uniformity (panel to panel and within a panel)	Primaries: < 0.015 radius Secondaries: <0.021 radius Gray scales: <0.021 radius
Chromaticity Red Green Blue White	$u' = 0.416/v' = 0.522$ $u' = 0.118/v' = 0.544$ $u' = 0.146/v' = 0.338$ $u' = 0.215/v' = 0.482$
Response time	<18ms at 25 deg C
Image retention	No retained images

<b>Design Parameters</b>	<b>ADC Performance (Ref. 3 &amp; 6)</b>
Outline dimensions	8.0 in. L x 5.5 in. W x 2.25 in. H
Connectors	3 External MIL-C-38999 Circular
Temperature Indicator	Externally mounted
Mounting Holes	4 in. x 0.189 diameter
Weight	2.5 lbs
Power dissipation	4.5 Watts (typical); 7.5 watts (Max)
Cooling	Conduction/Radiation
Chassis/Top and Bottom cover	Aluminum plate components
Input channel	25 Hz sampled rate
Data rate	To/From 1553B 3%

<b>Design Parameters</b>	<b>IDP Performance (Ref. 3 &amp; 6)</b>
Outline dimensions	18.0 in. L x 10.12 in. W x 7.62 in. H
Connectors	8 External MIL-C-38999 Circular 1 External NASA (MSFC) Circular
Temperature Indicator	Internally mounted Max
Weight	32 lbs
Power Dissipation	140 Watts Total includes 40 Watts for Growth
Cooling	Forced air with conduction/radiation
Chassis/Top and Bottom cover	Aluminum plate components
I/O Ports	6 one MHz, 32-bit word size, Manchester encoded, bi-phase, data bus interface.
Processor capabilities	2.0 MIPS
Memory	300 MB non-volatile internal mass storage. Transfer rate of 1.2 MB/s 1MB of EEPROM



## APPENDIX B. MATLAB PROGRAMS 'SHUTTLE' AND 'INIT'

### SHUTTLE

This program determines the impact point of a vehicle given an initial state vector. The dynamical equations of motion are based on Newton's law of motion,  $F=ma$ . Only the atmospheric phase of flight is assumed below. The equations and variables below are from Ref. 7, Ref. 11, Ref. 12 and Ref. 13. The data for the variables are extrapolated from various tables and graphs in these references.

---

These variables correspond to the initial state vector; position and velocity.  
 $x1=R$ ;  $x2=\lambda$ ;  $x3=C\lambda$ ;  $x4=R_p$ ;  $x5=\lambda_p$ ;  $x6=C\lambda_p$

function  $\dot{x} = shuttle(t,x)$

Variables below are picked so that the problem is over simplified for the purpose of illustration. The atmospheric density model used here is based on a two-parameter atmospheric model. It assumes that the atmospheric layer is isothermal.

$h=109400$ ;	Altitude (m)
$W_{io}=7.2921159e-5$ ;	Inertial Earth angular vel. (rad/sec)
$\rho_0=1.752$ ;	$kg/m^3$
$H=7.342e3$ ;	Scale Height (m) varies w/ altitude
$\rho=\rho_0 \cdot \exp(-h/H)$ ;	Density atmos. model ( $kg/m^3$ )
$C_d=0.25$ ;	Drag Coeff. varies dep. on configuration
$C_l=0.5$ ;	Lift Coeff. varies dep. on configuration
$S=600$ ;	Frontal Area of Shuttle + wings ( $m^2$ )
$M=12000$ ;	Mass of Orbiter (kg)
$B=10$ ;	Angle of Bank (degree) changed to rad in equations below.



These variables apply in cases where thrust is available.

$\Gamma=0;$	Mass flow rate of fuel ~ 374 kg/s per SSME
$V_e=0;$	Effective Vel of gases ~ 4465 m/s per SSME
$A_e=0;$	Engine gimbal angle about -ly axis
$A_d=0;$	Eng. gimbal angle about displaced lz axis

Atmospheric velocity

$V = [x(4) \ x(1)*(x(5)-W_{io})*\cos(x(3)) \ x(1)*x(6)]'$ ; magnitude of V

$V_{am} = \sqrt{x(4)^2 + [x(1)*\cos(x(3))*(x(5)-W_{io})]^2 + (x(1)*x(6))^2}$ ;

The forces herein are External specific forces (force per unit mass) assuming a no-wind condition and a continuum flow regime.

Drag Force

Drag forces are produced as a vehicle flies through the atmosphere. Dependent on atm. density, Surface area, and vehicle velocity.

$Z = -\rho * C_d * S / 2 * M * V_{am}$ ;

$rF_{dr} = Z * x(4)$ ;

$lF_{dr} = Z * x(1) * \cos(x(3)) * (x(5) - W_{io})$ ;

$LF_{dr} = Z * x(1) * x(6)$ ;

$F_{dr} = [rF_{dr} \ lF_{dr} \ LF_{dr}]'$ ;

### Lift Force

Dependent on atmospheric density, Surface area, and vehicle velocity.

$$Q = \rho * C_l * S * V_{am}^2 / M;$$

$$rFli = Q * \sqrt{V(2)^2 + V(3)^2} * \cos(B * \pi / 180);$$

$$lFli = Q * (V_{am} * V(3) * \sin(B * \pi / 180) - x(4) * V(2) * \cos(B * \pi / 180)) / \sqrt{V(2)^2 + V(3)^2};$$

$$LFli = -Q * (V_{am} * V(2) * \sin(B * \pi / 180) + x(4) * V(3) * \cos(B * \pi / 180)) / \sqrt{V(2)^2 + V(3)^2};$$

$$Fli = [rFli \ lFli \ LFli]';$$

### Thrust Force

Thrust forces for the shuttle before External Tank separation comes from the 3 SSMEs or the 2 OMS engines. The 3 cases are 3 engine out(EO), 2 EO or 1 EO.

$$Ah = \text{atan2}(V(3), V(2));$$

$$\gamma = \text{atan2}(V(1), \sqrt{V(2)^2 + V(3)^2});$$

$$rFth = -\Gamma * V_e / M * (\cos(A_e) * \cos(A_d) * \sin(\gamma) + \sin(A_d) * \cos(\gamma) * \sin(B) + \sin(A_e) * \cos(A_d) * \cos(\gamma) * \cos(B));$$

$$lFth = -\Gamma * V_e / M * (\cos(A_e) * \cos(A_d) * \cos(\gamma) * \cos(A_h) - \sin(A_d) * \sin(A_h) * \cos(B) - \sin(A_d) * \sin(\gamma) * \cos(A_h) * \sin(B) + \sin(A_e) * \cos(A_d) * \sin(A_h) * \sin(B) - \sin(A_e) * \cos(A_d) * \sin(\gamma) * \cos(A_h) * \cos(B));$$

$$LFth = -\Gamma * V_e / M * (\cos(A_e) * \cos(A_d) * \cos(\gamma) * \sin(A_h) + \sin(A_d) * \cos(A_h) * \cos(B) - \sin(A_d) * \sin(\gamma) * \sin(A_h) * \sin(B) - \sin(A_e) * \cos(A_d) * \cos(A_h) * \sin(B) - \sin(A_e) * \cos(A_d) * \sin(\gamma) * \sin(A_h) * \cos(B));$$

$$Fth = [rFth \ lFth \ LFth]';$$

## Gravity Force

These equations below take into account the oblateness of the earth and the distance from the Earth's center.

$$G_{sp}=3.9839e14/x(1)^2; \quad \text{Spherical grav. mass attrctn (m/sec}^2\text{)}$$

$$R_{eq}=6378338; \quad \text{Equatorial radius (m)}$$

$$rG=-G_{sp}+0.893e-3 \cdot G_{sp} \cdot (R_{eq}/x(1))^2 \cdot (1-3 \cdot \cos(2 \cdot x(3)));$$

$$IG=0;$$

$$LG=-1.638e-3 \cdot G_{sp} \cdot (R_{eq}/x(1))^2 \cdot \sin(2 \cdot x(3));$$

$$FG=[rG \ IG \ LG]^T;$$

-----

The state space formulations below are put in a form that can be easily integrated given an initial condition. Included in the formulation are the five part acceleration equation.

$$\dot{x}(1,1)=x(4);$$

$$\dot{x}(2,1)=x(5);$$

$$\dot{x}(3,1)=x(6);$$

$$\dot{x}(4,1)=x(1) \cdot x(6)^2 + x(1) \cdot x(5)^2 \cdot \cos(x(3))^2 + F_{dr}(1) + F_{li}(1) + F_{th}(1) + FG(1);$$

$$\begin{aligned} \dot{x}(5,1) = & 1/x(1)^2 / \cos(x(3))^2 \cdot (x(1) \cdot \cos(x(3))) \cdot (F_{dr}(2) + F_{li}(2) + F_{th}(2) + FG(2)) - 2 \\ & \cdot x(1) \cdot x(4) \cdot x(5) \cdot \cos(x(3))^2 - x(1)^2 \cdot x(5)^2 \cdot \cos(x(3)) \cdot (-\sin(x(3))) \cdot x(6); \end{aligned}$$

$$\begin{aligned} \dot{x}(6,1) = & 1/x(1) \cdot (-2 \cdot x(4) \cdot x(6) - x(1) \cdot x(5)^2 \cdot \cos(x(3)) \cdot \sin(x(3))) + F_{dr}(3) + F_{li}(3) + F_{th}(3) + FG(3); \end{aligned}$$

## INIT

This program plots and outputs the impact point geocentric latitude and longitude.

### Constants;

Re=6378140;	Earth radius (m)
Wio=7.2921159e-5;	Earth angular velocity (radians/sec)

### Variables;

t0=0;tf=1000;	Time varies the tf to get alt to ~zero
h=109400;	Altitude (m)~359,000 ft, nominal alt after External Tank separation

An Initial Condition/Initial state vector input is needed for numerical analysis. This is assuming 22 deg North Latitude and 67.3 deg West Longitude at 359,000 feet. Obviously this can be moved to any initial position. The initial velocity vector only has an easterly component for purpose of illustration.

### Position ;

R0=Re+h;	m, init. dist. from Earth cntr
l0=-67.3*pi/180;	rad, 0 deg Longitude
L0=22*pi/180;	rad, 0 deg Latitude

### Velocity (relative);

Rpinit=0;	ft/s, radial component
lpinit=22490;	ft/s, Longitudinal component
Lpinit=3996;	ft/s, Latitudinal component

Rp0=Rpinit*pi/60/5280/180;	converts ft/s to rad/s
lp0=lpinit*pi/60/5280/180;	converts ft/s to rad/s

```
Lp0=Lpinit*pi/60/5280/180;      converts ft/s to rad/s
x0=[R0 l0 L0 Rp0 lp0 Lp0]';      IC column vector
```

```
2nd,3rd order integrator;
[t,x]=ode23('shuttle',t0,tf,x0);
```

This loop determines the index value which contains the altitude value closest to zero. This is an approximation used only for the purpose of illustration.

```
for i=1:length(x)
    if (x(i,1)<6391000) & (x(i,1)>6358000)
        k=i;
    end
end
```

This determines the altitude, geocentric Lat & Long for plotting.

```
Alt=(1/1000*x(1:k,1))-6378;
Longitude=(x(k,2)-Wio*t(k))*180/pi
Latitude=x(k,3)*180/pi
```

Plotting routine which plots the Altitude vs. time and the Latitude vs. Longitude.

```
subplot(211),plot(Longitude,Latitude,'o'),grid,ylabel('Lat      (deg)'),xlabel('Long
(deg)'),title('Lat vs. Long')
subplot(212),plot(t(1:k),Alt),grid,ylabel('Altitude(km)'),xlabel('time(s)'),title('Alt
vs. t')
```

## INITIAL DISTRIBUTION LIST

1. Defense Technical Information Center.....2  
     Cameron Station  
     Alexandria, Virginia 22304-6145
  
2. Dudley Knox Library.....2  
     Code 052  
     Naval Postgraduate School  
     Monterey, California 93943-5101
  
3. Chairman, Code AA.....1  
     Department of Aeronautics and Astronautics  
     Naval Postgraduate School  
     Monterey, California 93943-5002
  
4. Chairman, Code SP.....1  
     Space Systems Academic Group  
     Naval Postgraduate School  
     Monterey, California 93943-5000
  
5. CDR. Wade D. Duym, Code 31.....1  
     Aerospace Engineering Curricular Office  
     Naval Postgraduate School  
     Monterey, California 93943-5107
  
6. Dr. Conrad F. Newberry, Code AA/NE.....3  
     Space Systems Academic Group  
     Naval Postgraduate School  
     Monterey, California 93943-5000
  
7. Dr. Sandy Scrivener, Code AA.....1  
     Space Systems Academic Group  
     Naval Postgraduate School  
     Monterey, California 93943-5000
  
8. Curricular Officer, Code 37.....1  
     Naval Postgraduate School  
     Monterey, California 93943-5000

9. CAPT. Thompson.....1  
Office of the Chief of Naval Operations  
Code N63, Room 4E679 The Pentagon  
Washington, DC 20350-20000
  
10. Commander, Naval Space Command.....1  
ATTN: N112  
5280 4th Street  
Dahlgren, Virginia 22448-5300
  
11. CDR. Kent Rominger.....2  
Mail Code CB  
NASA, Johnson Space Center  
Houston, Texas 77058
  
12. Major Chris Hadfield.....1  
Mail Code CB  
NASA, Johnson Space Center  
Houston, Texas 77058
  
13. LCDR. Brent Jett.....1  
Mail Code CB  
NASA, Johnson Space Center  
Houston, Texas 77058
  
14. Sergio Carrion.....1  
Rockwell International Corp., STS Division  
12214 Lakewood Blvd.  
Downey, California 90241
  
15. Diana Schuler.....2  
Mail Code EV132  
NASA, Johnson Space Center  
Houston, Texas 77058
  
16. Richard Mastracchio.....1  
Mail Code DM431  
NASA, Johnson Space Center  
Houston, Texas 77058
  
17. LT. Baoquoc Tranthien, USN.....2  
734 Covina Way  
Fremont, California 94539